Facies (2005) 50:443–462
DOI 10.1007/s10347-004-0027-4

ORIGINAL PAPER

Eberhard Gischler · Anthony J. Lomando

Offshore sedimentary facies of a modern carbonate ramp, Kuwait, northwestern Arabian-Persian Gulf

Received: 7 May 2004 / Accepted: 17 September 2004 / Published online: 16 November 2004

Abstract The Kuwait example studied here may serve as a model for ancient carbonate ramp systems just as the classical—but markedly different—southern Arabian-Persian Gulf ramp of the Trucial Coast (United Arab Emirates). Five sedimentary facies may be distinguished on the modern southern Kuwait carbonate ramp based on quantitative sedimentological, mineralogical, and geochemical analyses of 130 surface sediment samples and by using multivariate statistics. These facies include (1) inner ramp ooid-skeletal grainstone with common aggregate grains, peloids, and molluscs, (2) limited occurrences of nearshore quartz-ooid sand, (3) mid ramp mollusk packstone to grainstone, (4) outer ramp mollusk-marl wackestone with abundant siliciclastic fines, and (5) coralgal grainstone that is found on small nearshore patch reefs and outer ramp pinnacle and platform reefs. In addition to facies (1), an aggregate grain packstone to grainstone sub-facies is mapped out where abundances of this grain type exceed 20%. Ooid-skeletal grainstone, mollusk packstone to grainstone, and coralgal grainstone are predominantly aragonitic with 5–10% insoluble residue on average. Mollusk-marl wackestone has 55% insoluble residue on average with aragonite and low-magnesium calcite predominating in the carbonate fraction. Dolomite in this facies is interpreted to be of eolian origin derived from the upwind deserts of Syria and Iraq. Facies distribution is correlated with water depth, and hence controlled by depositional energy, primarily wavebase. This correlation is seen in the results of statistical analyses and in the fact that facies boundaries are more or less parallel to depth contours. Ooid-skeletal grainstones are found in depths from 0 to <10 m. The boundary between the mollusk packstone to grainstone and the mollusk-marl wackestone, which also marks the transition from grain-supported to mud-supported textures, is situated between 15–20 m depth and is much sharper than the boundary between the ooid-skeletal and the mollusk packstone to grainstone facies. Carbonate-dominated facies may also be distinguished geochemically as indicated by significantly different carbon and oxygen isotope compositions. The latter should be kept in mind when using bulk isotope values for chemostratigraphy or for paleo-environmental reconstructions in fossil carbonate ramps and platforms.

Keywords Ramp · Holocene · Kuwait · Arabian-Persian Gulf · Carbonate sediments

E. Gischler (✉)
Geologisch-Paläontologisches Institut,
Johann Wolfgang Goethe-Universität,
Senckenberganlage 32, 60054 Frankfurt am Main, Germany
e-mail: gischler@em.uni-frankfurt.de
Tel.: +49-69-79825136

A. J. Lomando
ChevronTexaco,
Kuwait Pouch,
93 Wigmore Street, London, W1U 1HH, UK

Introduction: previous studies and purpose

The southwestern coast of the Arabian-Persian Gulf, in particular the United Arab Emirates (UAE) and offshore areas, has been the focus of studies in marine carbonate sedimentology for nearly half a century. In a pilot study, Emery (1956) investigated texture and mineralogy of small quantities of offshore surface sediments, adhering to the tallowed sounding leads used in early hydrographic surveys of the entire area. Surface sediments including distribution of benthic foraminifera of the area surrounding the Qatar Peninsula were studied in detail by Houbolt (1957). Following this work, a large number of sedimentological studies—of which only the major ones are cited here—concentrated on the southern area of the Arabian-Persian Gulf, namely the UAE (e.g., Evans et al. 1964; Evans 1966; Kinsman 1969; Kendall and Skipwith 1969). Likewise, Purser (1974) edited the results of a large number of sedimentological, mineralogical, ecological, and hydrographical studies from the UAE and nearby offshore areas around Qatar and Bahrain. Modern offshore sediment types and their distribution were described by Wagner and Van der Togt (1973), who delineated 14 carbonate (skeletal and non-skeletal) and non-

carbonate types in that same area. The southern Arabian-Persian Gulf usually serves as a model of ramp depositional settings in general (e.g., Ahr 1973, 1998; Burchette and Wright 1992; Kirkham 1998). However, this view was recently questioned by Walkden and Williams (1998), who pointed out the fact that the Arabian Gulf carbonate system is in tectonic, eustatic, and depositional disequilibrium, and was emergent for most of the past ca. 2.5 Ma.

In contrast to the intensively studied southern areas, the northwestern parts of the Arabian-Persian Gulf have received less attention, even though the general setting is significantly different (Gunatilaka 1986). Whereas the UAE coast is characterized by barrier-type shoals oriented perpendicular to the prevailing wind with leeward protected mud-dominated lagoons, the northwestern Gulf is unprotected and winds blow parallel to the coast (Lomando 1998). Studies of modern offshore sediments in the northwestern Gulf have concentrated largely on clay and carbonate mineralogy and texture, and identified three sources of sediment: dust storms in southern Iraq and in Kuwait, river input from the Euphrates and Tigris rivers, and the marine carbonate system (Khalaf and Ala 1980; Khalaf et al. 1982; Al-Bakri and Al-Ghadban 1984; Al-Ghadban 1990; Al-Sarawi et al. 1993). Aspects of carbonate sedimentology and facies were described by Khalaf et al. (1984). These authors claimed that carbonate sediment components are dominated by mollusk shells and shell fragments, foraminiferal tests, and echinoid skeletal parts whereas non-skeletal grains such as ooids and peloids were observed only occasionally and therefore were not quantified (Khalaf et al. 1984: 540–541 and their Fig. 10). Even so, during our own reconnaissance work we observed abundant non-skeletal grains such as ooids, aggregate grains, and peloids in submarine sediments collected offshore southern Kuwait, especially within the inner ramp area. Even though Khalaf et al. (1984: 535 and their Fig. 1) give no information on sample locations but only sampling zones, we presume that these authors did not sample the inner ramp area.

Our study was designed to detail carbonate facies of the southern Kuwait ramp system in order to (1) revise the facies patterns as described by Khalaf et al. (1984), (2) contribute to the knowledge of carbonate sedimentology of the northern Arabian-Persian Gulf area in particular, and (3) enhance the knowledge and understanding of the sedimentology of the Gulf in general, which serves as a modern analogue for many ancient ramp depositional settings, but largely based on studies in its southern (UAE) part.

Setting

The climate in the study area is hot and arid with air temperature maxima of up to 52 °C in July-August and minima of around 13 °C in January. However, temperatures close to freezing have been recorded. Annual precipitation rates reach 115 mm/year. The wind blows from the NW ("Shamal") for most of the year, and to a lesser extend from the SE ("Kaus") (Khalaf 1988). In combination with the counterclockwise tidal currents and the predominating winds, water currents mostly run parallel to the coast (Gunatilaka 1986). The tidal range is 2.5–3.0 m (Khalaf 1988). Water temperatures range from 13–32 °C and salinities fluctuate between 38.5–42.5‰ around the Kuwait offshore reef islands (Downing 1985).

The study area lies in the northernmost Arabian-Persian Gulf, offshore southern Kuwait (Figs. 1, 2). Whereas the offshore area east of Kuwait City deepens over a relatively short distance from the shoreline to 20 m water depth and is dominated by siliciclastic sedimentation due to the proximity to the Euphrates-Tigris major deltaic complex (e.g., Baltzer and Purser 1990), the southern area off Kuwait has a homoclinal ramp morphology (Read 1985) with carbonate sedimentation predominating (Gunatilaka 1986). Away from the shoreline, water depths increase to a maximum of 35 m some 40 km offshore. Following the review by Burchette and Wright (1992), we distinguish between inner ramp (0–7.5 m water depth), mid ramp (7.5–17 m), and outer ramp (>17 m) environments in the study area.

The shoreline of the study area is characterized by the two prominent headlands of Ras Al-Julayah and Ras Al-Zour. Quaternary cemented beach deposits including modern beachrock are common along the shore (Khalaf 1988). Picha (1978), Gunatilaka (1991), Robinson and Gunatilaka (1991), and Duane and Al-Zamel (1999) described some aspects of the sabkhas in the area east of Al-Khiran including modern dolomite and microbial mats. Lomando (1999) discussed the influence of structure on modern facies patterns including sabkhas, coastal ridge and dune complexes, and shallow subtidal shoals.

Several pinnacle-like carbonate shoals with low-diversity reefs (Downing 1985; Carpenter et al. 1997) occur on the outer ramp the most prominent of which have small sand cays named Kubbar, Qaro, and Umm Al-Maradem (Fig. 2). Qaro is also the site of submarine oil seepage (Uchupi et al. 1996). As yet, there is no data on reef foundations, which could include diapire structures as in the southern Gulf, tectonic highs, or Pleistocene reefs. A number of very small, low-diversity coralgal patch reefs are also found in the inner ramp environment. High turbidity, elevated salinity, and significant fluctuations in water temperatures are the principle stresses on these reefs (Carpenter et al. 1997). Two distinct reef trends can be found (Fig. 1). In the nearshore reef trend, a series of six small patch reefs occur in water depths of 10 m or less. These are characterized by massive *Porites* and brain corals such as *Platygyra*, oysters, and other bivalves. The higher turbidity in nearshore areas tends to restrict the size and diversity of these patch reefs in comparison to the offshore trend. Most of the offshore reef buildups rise up from a seabed of 25–30 m depth. Umm Al-Aysh (Taylor's Rock) and Mudayrah are buildups whose tops are never exposed at low tide. Mudayrah is a cluster of patch reefs on a flat-topped structure whereas Umm Al-Aysh is a single pinnacle. The best-

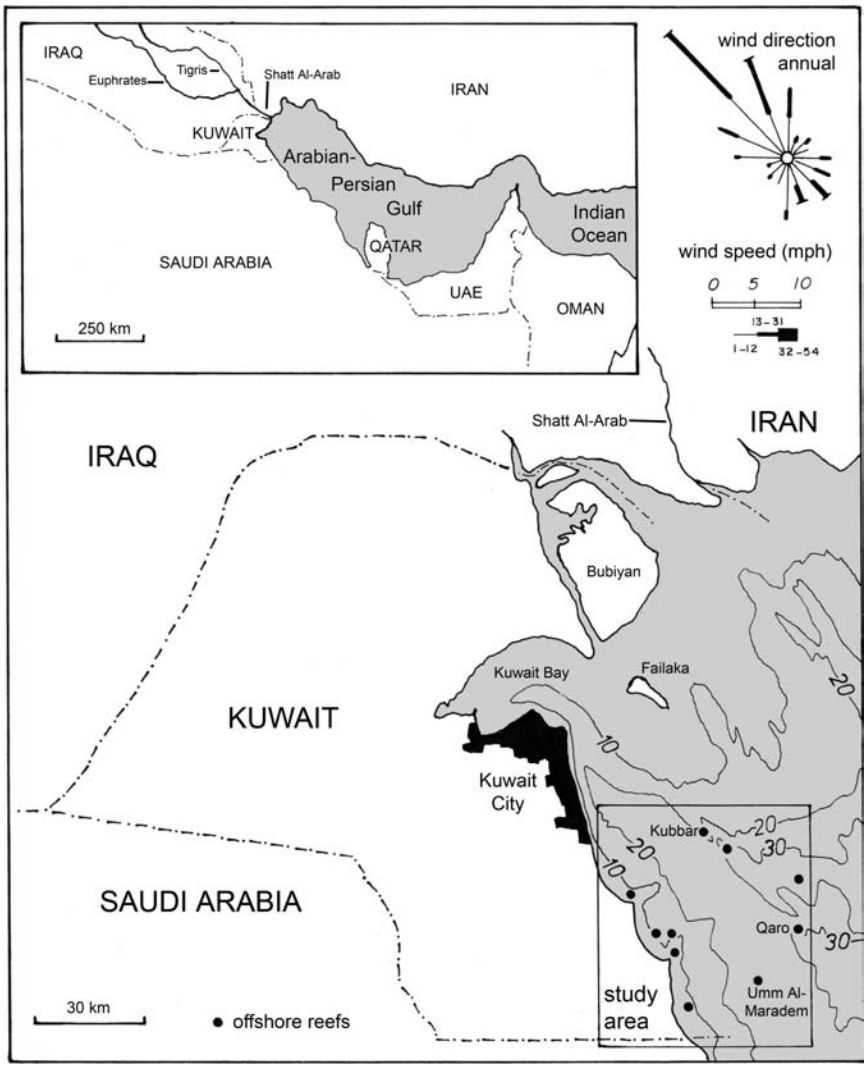

Fig. 1 Map of Kuwait, northwestern Arabian Gulf and the study area. Wind data from Khalaf (1988). *Depth contours* are in meters. Kubbar, Qaro, and Umm Al-Maradem are reef-fringed, low-lying sand islands

developed coral reefs are the offshore reefs at Umm Al-Maradem, Qaro, and Kubbar**,** which all have vegetated skeletal sand islands. Significant coral development occurs above a depth of 15 m but most coral growth occurs above 10 m. Corals, algae, mollusks, crustaceans, sponges, echinoderms, and polychaetes in addition to abundant fish make up the general reef communities (Downing 1985; Carpenter et al. 1997). The carbonate secreting organisms in these communities produce significant sediment ranging from fine sand to cobble size, which feed the cay beaches, reef sand flats and reef slopes.

Kubbar will serve as an example of an offshore reef-island complex (Fig. 3). Kubbar reef is elliptical in shape, about 1.5 km long and 1 km wide. The reef communities are less diverse than those found on southern reefs but the overall reef-island complex is representative of all the occurrences. The northernmost location of Kubbar may be responsible for the lower coral diversity. This reef platform location is northernmost and therefore closest to the Shatt al Arab, which causes higher water turbidity and increased stress in comparison to reefs farther south.

The reef flat area is dominated by *Porites* and accessory brain corals such as *Platygyra*, and some *Acropora*. A series of small non-emergent patch reefs occurs to the north and northwest of Kubbar, separated from the main reef-island complex by a series of sand-rich channels. The reef slope passes rapidly from coral growth to a coarse debris apron. The toe-of-slope is dominated by very coarse debris mixed with green marl and abruptly passes into marl-wackestone at a depth averaging 20 m. Kubbar Island is about 500 m long and is encircled by extensive beach and beachrock. Kubbar has the highest elevation of islands on the Kuwait reef platforms. An extensive raised terrace, which is approximately 4 m above modern sea-level, encircles a central depression. This raised terrace was perhaps developed during an older phase of island building when Holocene sea-level was higher, and it may be correlated with terraces and ridges on the Kuwait coast, which are up to 4 m above modern sea-level and exhibit an age range from 5,500–2,300 k.y. BP (Gunatilaka 1986). On the windward and flanking portions of the terrace is a crescent-shaped vegetated (stabilized) eolian dune rim composed of rooted, very fine skeletal sand and

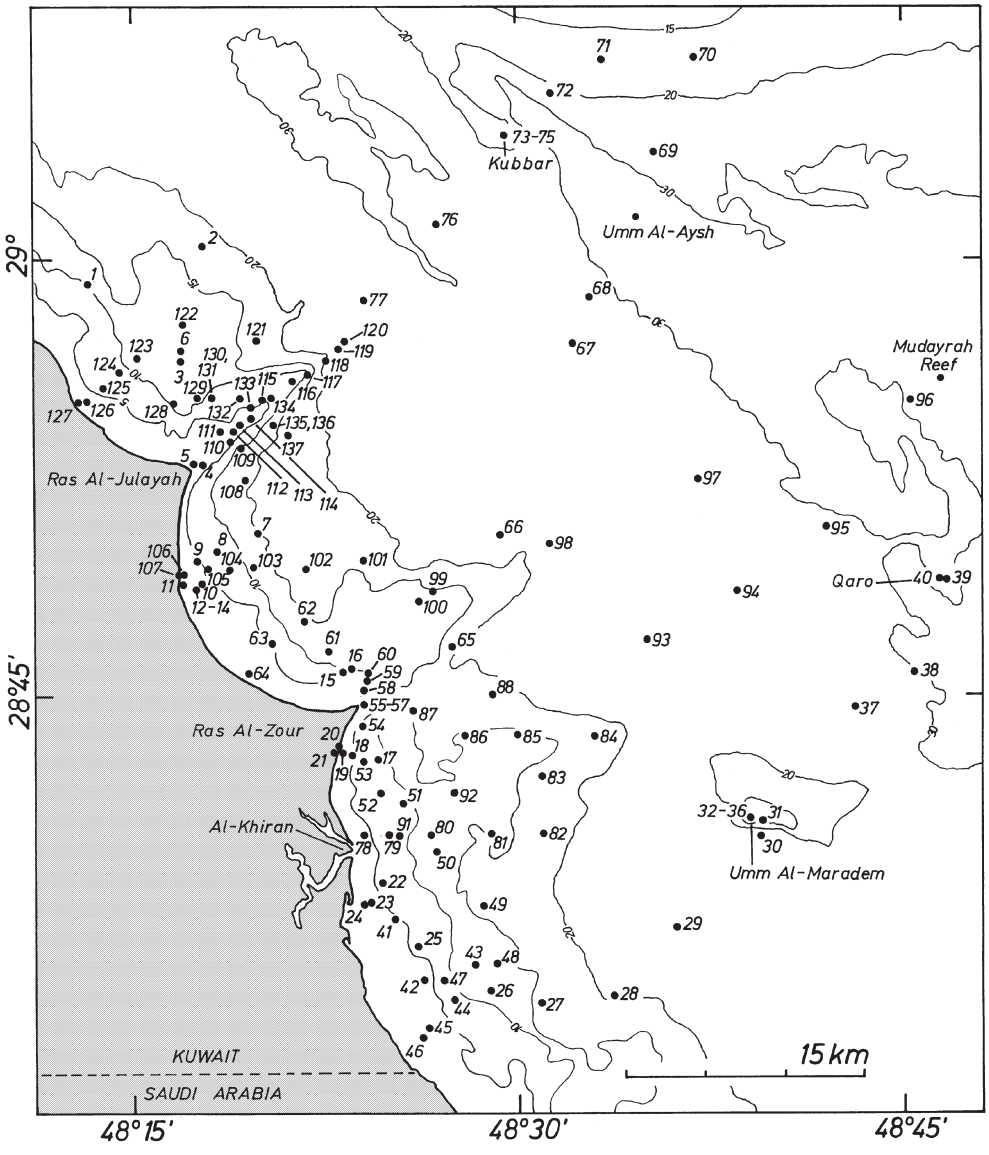

Fig. 2 Map of the study area showing the sample points. *Depth contours* are in meters. Map is based on British Admirally Chart 3773

silt. Intertidal beachrock occurs in windward (northwest) and leeward locations. The windward beachrock is less well developed and has distinctive large beachrock slabs and boulders thrown up to higher beach elevations by major storms. In contrast, the leeward beachrock is a very extensive shingled deposit. Development and preservation of this leeward extensive beachrock deposit is caused by two factors. Wave refraction around the island promotes beachrock formation. The leeward position inhibits erosion through its protected setting.

Methods

From October-December 2001 and in June 2002, we collected a total of 130 surface sediment samples offshore southern Kuwait (Fig. 2) using a Lenz-type sampler (Hydrobios, Kiel, Germany) operated from small boats. The rope attached to the sampler was marked every meter in order to measure water depth during sampling. We determined sample locations using GPS. At shallow locations, approx. less than 5 m water depth, we made observations with regard to bottom type and biota by snorkeling. Offshore sediment samples were washed in a dilute solution of Clorox, dried in an oven at 40 °C, and sieved into the common size-classes >2, 2–1, 1–0.5, 0.5–0.125, 0.125–0.063, and <0.063 mm. Deeper water samples, which contained approx. >50% fine grain-sizes (<0.125 μm) were wet-sieved. Size-fractions were then weighed. Sub-samples from the size-fractions >125 μm of individual samples were obtained by use of a sample-splitter, filled in ice cube trays, and impregnated with epoxy resin. These billets and additional four beachrock samples were cut, polished, and thin-sectioned. Thin-sections then investigated with a petrographic microscope. In addition, four beachrock samples from offshore carbonate islands were studied in thin-sections. Composition was quantified by counting 200 grains per thin-section using a point-counter. We used 125 μm as minimum grain-size for thin-sectioning as identification and distinction of a number of constituent grains such as corals and mollusks, are not readily possible under the microscope below this size. Grain-sizes <125 μm are designated as "mud" in the following. The size-fraction <63 μm was qualitatively investigated in four samples under SEM. Carbonate contents of pulverized bulk samples were determined using a Scheibler-type calcimeter. X-ray diffractometry (Phillips PW 1050, 40 kV, 20 mA, Cu-cathode) was

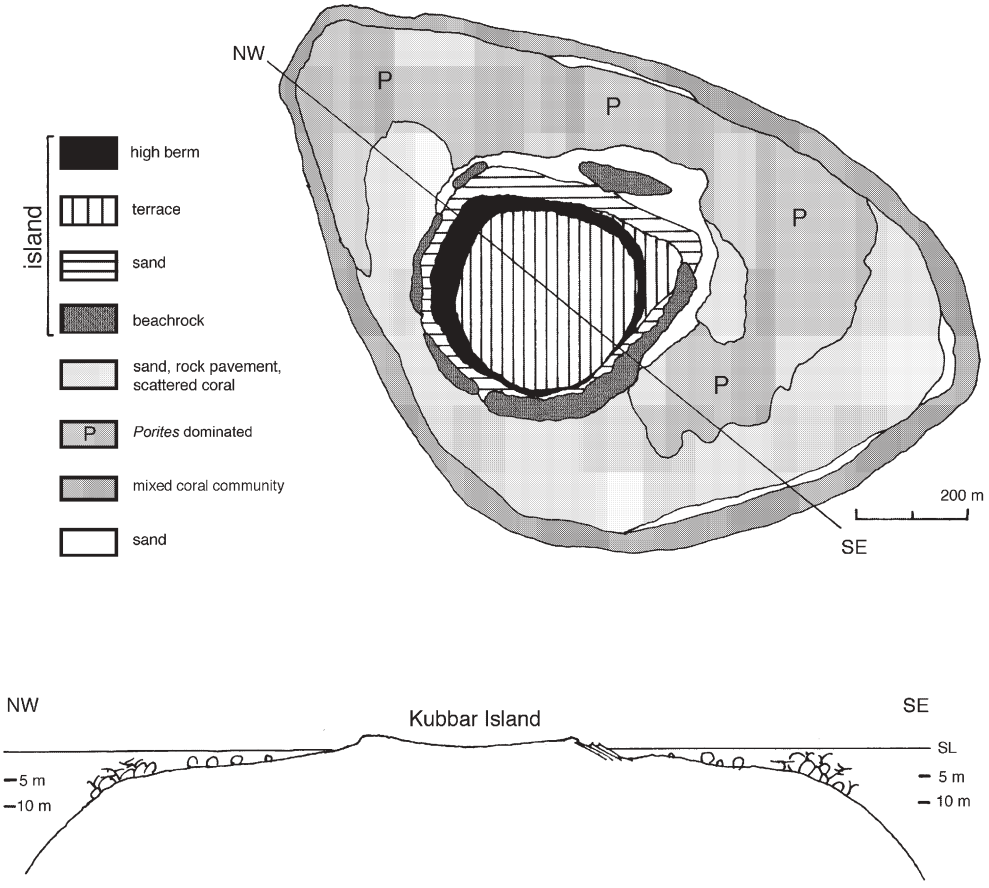

Fig. 3 Map and cross-section through the Kubbar reef complex. Based on unpublished data of the Kuwait Institute of Scientific Research

used to determine the mineralogy of samples (Milliman 1974: 22–29). According to the experienced operator, the accuracy of relative amounts of carbonate minerals is 5%. In order to identify clay minerals, carbonate was removed by a dilute solution of hydrochloric acid. The insoluble residue was then analyzed using X-ray diffractometry. We investigated a total of 92 carbonate-rich bulk samples and 14 samples of compositional end members (corals, mollusks, foraminifera, ooids, peloids, echinoderms) for stable isotopes of oxygen and carbon with a ThermoFinnigan MAT 253 mass spectrometer with gas bench and cryofocus. In order to delineate sedimentary facies, correlation analysis, cluster analysis, and factor analysis were performed using textural and compositional data (program Statistica).

Results

Sediment components and matrix

Carbonate components >125 μm include skeletal grains such as mollusk (largely bivalve and gastropod) shells and shell fragments, fragments of coral and red coralline algae, benthic foraminifera, and echinoderm fragments (Figs. 4, 5). Non-skeletal grains identified are ooids, peloids, and aggregate grains. Quartz was the only siliciclastic component quantified. Feldspar was observed very rarely.

The mud (<125 μm) consists of both fine-grained carbonate and siliciclastics as observed in the grain-size fraction <63 μm. Small quartz and feldspar grains, clay minerals illite, kaolinite, and smectite, as well as palygorskite make up the siliciclastic fines. Systematic data on clay minerals in the study area will be published elsewhere. Carbonate fines include small fragments of skeletal and non-skeletal origin as well as aragonite needles and nanograins (Fig. 6). Needles and nanograins may be derived from the breakdown of larger constituent grains or from direct precipitation, because codiacean algae such as *Halimeda* and *Penicillus* —as potential carbonate mud producers—do not occur in the study area. Based on trace element investigations of strontium, Kinsman (1969) and Loreau (1982) explained aragonite muds in Trucial Coast lagoons largely as inorganic precipitates, although an indirect bacterial influence on precipitation was not ruled out.

The distribution of constituent particles and the fine sediment (mud) is shown in cross-sections on Fig. 7. Non-skeletal grains mostly occur in the shallow inner ramp. Quartz is restricted to nearshore areas especially in the northern part of the study area. Mollusks are most common in intermediate depths of the mid-ramp environment. Deep outer ramp areas are predominated by marl. Mollusks may also be common locally in this environment.

Carbonate mineralogies include aragonite, high-Mg-calcite, low-Mg-calcite, and dolomite. Aragonite abundance decreases with increasing water depths (Fig. 8a) whereas abundances of high-Mg-calcite and low-Mg-calcite increase towards deeper water (Fig. 8b, c). Ele-

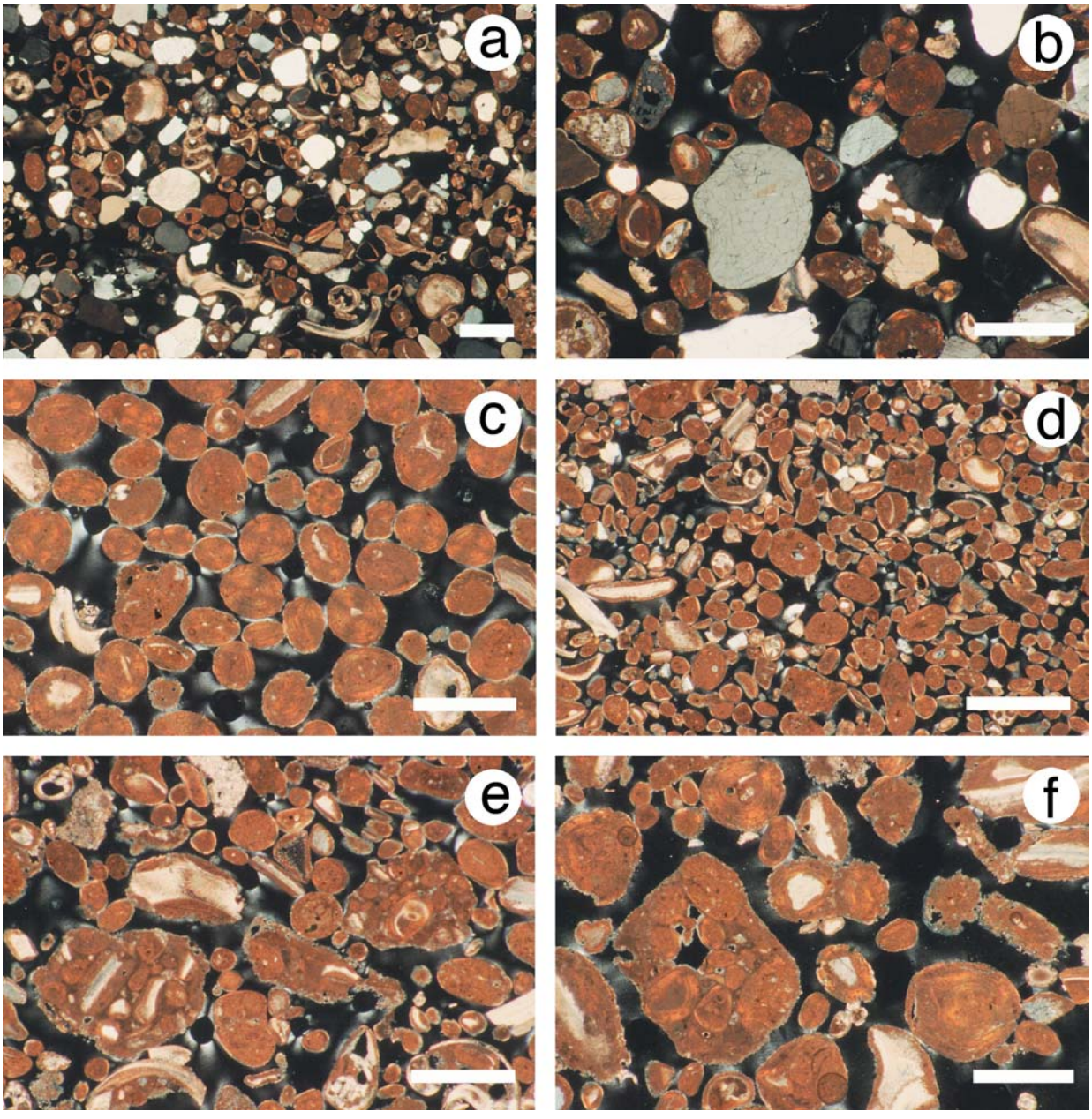

Fig. 4 Thin-section photographs of characteristic facies. All photos with crossed polars. *Scale bar* in all photos is 100 µm. **a** Quartz-ooid sand facies with rounded quartz grains, mollusk shell fragments, and ooids. Sample 005. **b** Quartz-ooid sand facies showing well rounded quartz grains and some ooids. Sample 004. **c** Ooid-skeletal grainstone facies with ooids predominating. Sample 041. **d** Ooid-skeletal grainstone facies with abundant peloids, some ooids and mollusk shell fragments, and few quartz grains. Sample 020. **e** Ooid-skeletal grainstone facies with aggregate grains, some mollusk shell fragments and peloids. Sample 019. **f** Ooid-skeletal grainstone facies with aggregate grains, ooids, and mollusk shell fragments. Sample 014

vated percentages of dolomite predominantly occur in the outer ramp settings and highest values are reached in the northern part of the study area (Fig. 8b). Dolomite is presumed to be detrital and of eolian origin. The abundance of insoluble residue, which includes fine quartz and clay minerals increases towards deeper water and towards the northern part of the study area (Fig. 8d).

Sedimentary facies

Delineation of five sedimentary facies was done based on applying a number of statistical analyses using compositional, textural, and mineralogical data, and water depth. The correlation matrix (Table 1) shows that the abundance of the majority of grain types, fine-grained sediment, insoluble residue, and carbonate mineralogy is significantly correlated with water depth, which is taken as a measure of depositional energy. Carbonate mineral-

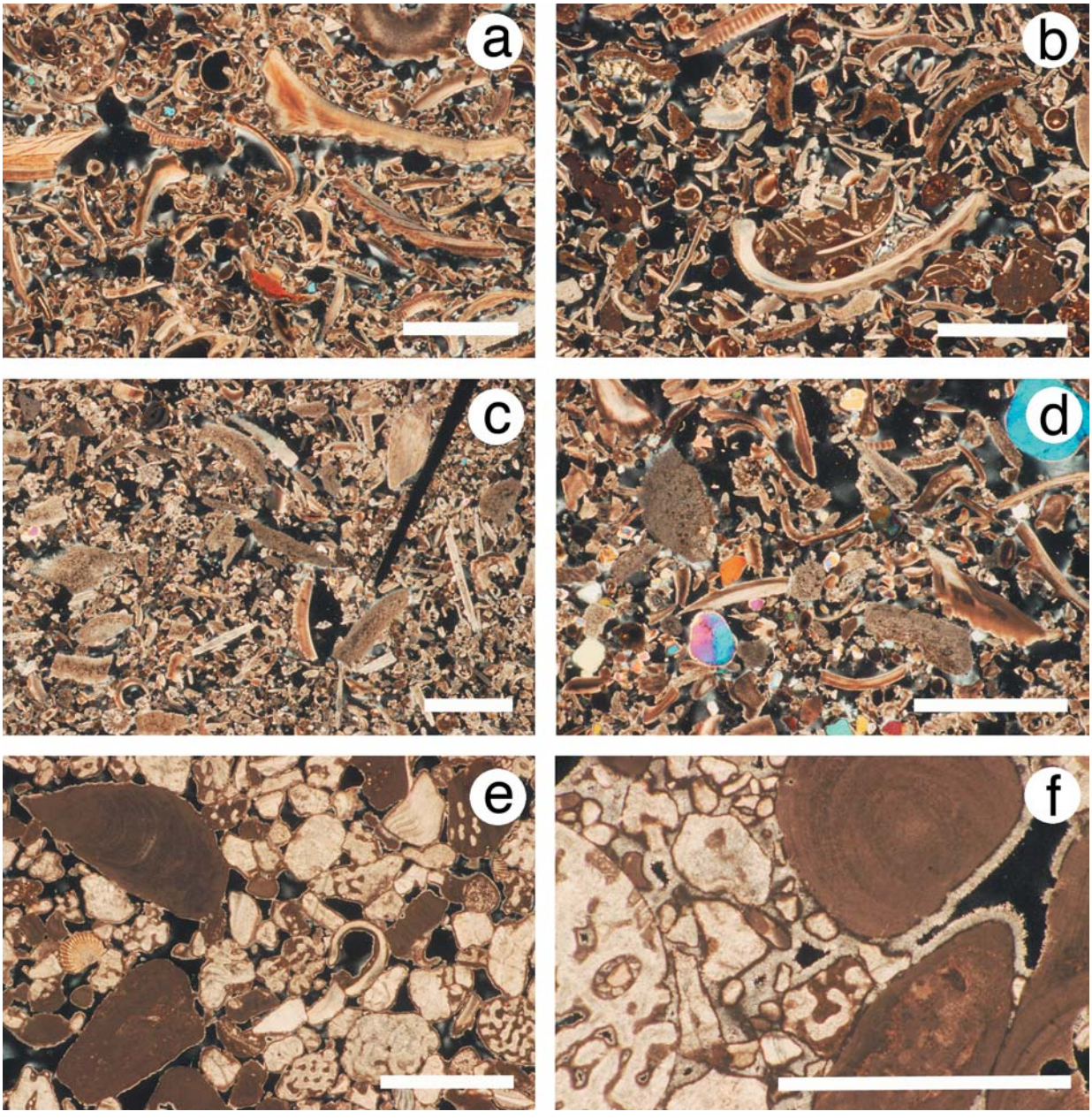

Fig. 5 Thin-section photographs of characteristic facies. All photos with crossed nichols. *Scale bar* in all photos is 250 μm. **a** Mollusk packstone to grainstone facies with abundant gastropod and pelecypod shells and shell fragments. Sample 001. **b** Mollusk packstone to grainstone facies with abundant gastropod and pelecypod shells and shell fragments. Note aggregate grains. Sample 086. **c** Mollusk marl wackestone facies with abundant mollusk shell fragments, echinoderm fragments, and few foraminiferal tests, as well as sponge spicule. Sample 028. **d** Mollusk marl wackestone facies exhibiting mollusk shell and echinoderm fragments, foraminiferal tests, and quartz grains. Sample 029. **e** Coralgal facies as seen in beachrock. Coral, red algal, mollusk, and echinoderm fragments cemented together by thin isopachous cement crust. Note micrite envelopes. Sample 036 (Kubbar Island). **f** Coralgal facies as seen in beachrock. Coral and red algal fragments cemented together by isopachous crust of aragonite needle cement. Sample 036 (Kubbar Island)

ogy is correlated—not surprisingly—with common grain types. The data matrix also shows significant correlations between certain grain types and indicates common occurrence in the study area. Corals and red algae exhibit correlations similar to those between mollusks and foraminifera and echinoderms, or ooids, or quartz. The results of an r-mode cluster analysis are shown on Fig. 9. It confirms the general picture as seen from the correlation analyses in that certain grain types form joint clusters. These include the well-defined groups corals-red algae, mollusks-foraminifera-echinoderms, and mud. Ooids, peloids, aggregate grains, and quartz form another dendrogram entity with ooids and peloids showing highest similarity and quartz exhibiting lowest similarity with the other three types. A factor analysis produced four factors that explain 73.5% of the total variance (Table 2). Scat-

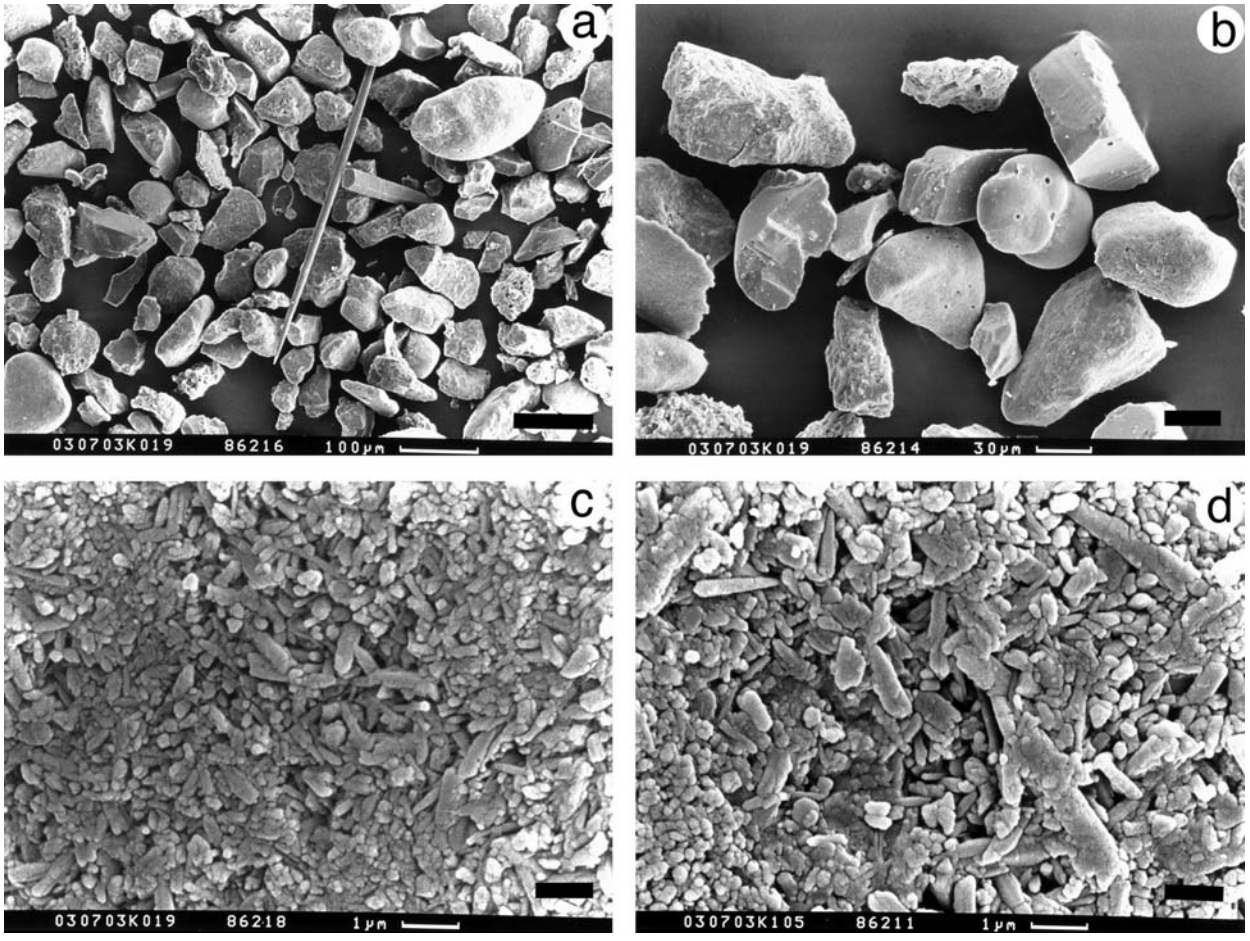

Fig. 6 SEM-photographs of fine sediment. **a** Grain-size fraction 63–20 μm. Angular fragments of mollusk shells, few peloids, and sponge spicule. Sample 019. *Scale bar* is 100 μm. **b** Grain-size fraction 63–20 μm. Angular mollusk shell fragments and foraminifer test. Sample 019. *Scale bar* is 30 μm. **c** Grain-size fraction <20 μm. Largely nanograins and few short needles of aragonite. Sample 019. *Scale bar* is 1 μm. **d** Grain-size fraction <20 μm. Aragonite needles and nanograins. Note that some needles are composed of nanograins. Sample 105. *Scale bar* is 1 μm

terplots using factors 1–3 (explaining 62.9% of the total variance) show good separations into five herds (Fig. 10).

Applying Dunham (1962) texture categories to these sediments (cf. Enos and Sawatsky 1981), five sedimentary facies are discerned (Fig. 11): quartz-ooid sand, ooid-skeletal grainstone, mollusk packstone to grainstone, mollusk marl wackestone, and coralgal grainstone. For practical reasons we shifted Dunham's upper grain-size limit for mud from 20 to 125 μm. Our inner ramp and reefal grainstones contain <1% mud on average and are clearly grain-supported. The outer ramp wackestones have >75% mud on average and are mud-supported. According to Dunham (1962) the transition from grain-supported to mud-supported lies between 35–70% mud depending on grain shape. The content of mud in our mid ramp packstones to grainstones has a high variability and ranges from 0–42.8% with an average value of 7.4%. These sediments are grain-supported.

Quartz-ooid sand.- This facies only occurs in close vicinity to the coast along a thin coastal ribbon from the point of Ras Al-Julayah northward (Figs. 4a, b, 11). The facies is defined by high quartz contents averaging 44% abundance (Table 3). Likewise, and as mud content is very low, content of insoluble residue averages 45%, including quartz nuclei of ooids and quartz in aggregate grains, in addition to free quartz sand. Apart from quartz grains, ooids, aggregate grains, and mollusk fragments are common with ooids being most abundant (average 21.3%). As a consequence, aragonite is the most abundant carbonate mineralogy (80–96%).

Ooid-skeletal grainstone.- This is the most common facies in the inner ramp with non-skeletal grains such as ooids, peloids, and aggregate grains being most abundant (Fig. 4c–e; Table 4). The facies covers a 2–7-km-wide stretch of sea floor from the coast to water depths <7.5 m (Fig. 11). Only two samples fall out of this bathymetric range. Near the Ras Al-Julayah and Ras Al-Zour headlands, ooid shoals and sandwaves are developed (Lomando 1999). The average value of non-skeletal grains amounts to 57.5% with ooids being the most abundant type (average 33.9%) and peloids being least abundant (average 8.9%). The average abundance of ag-

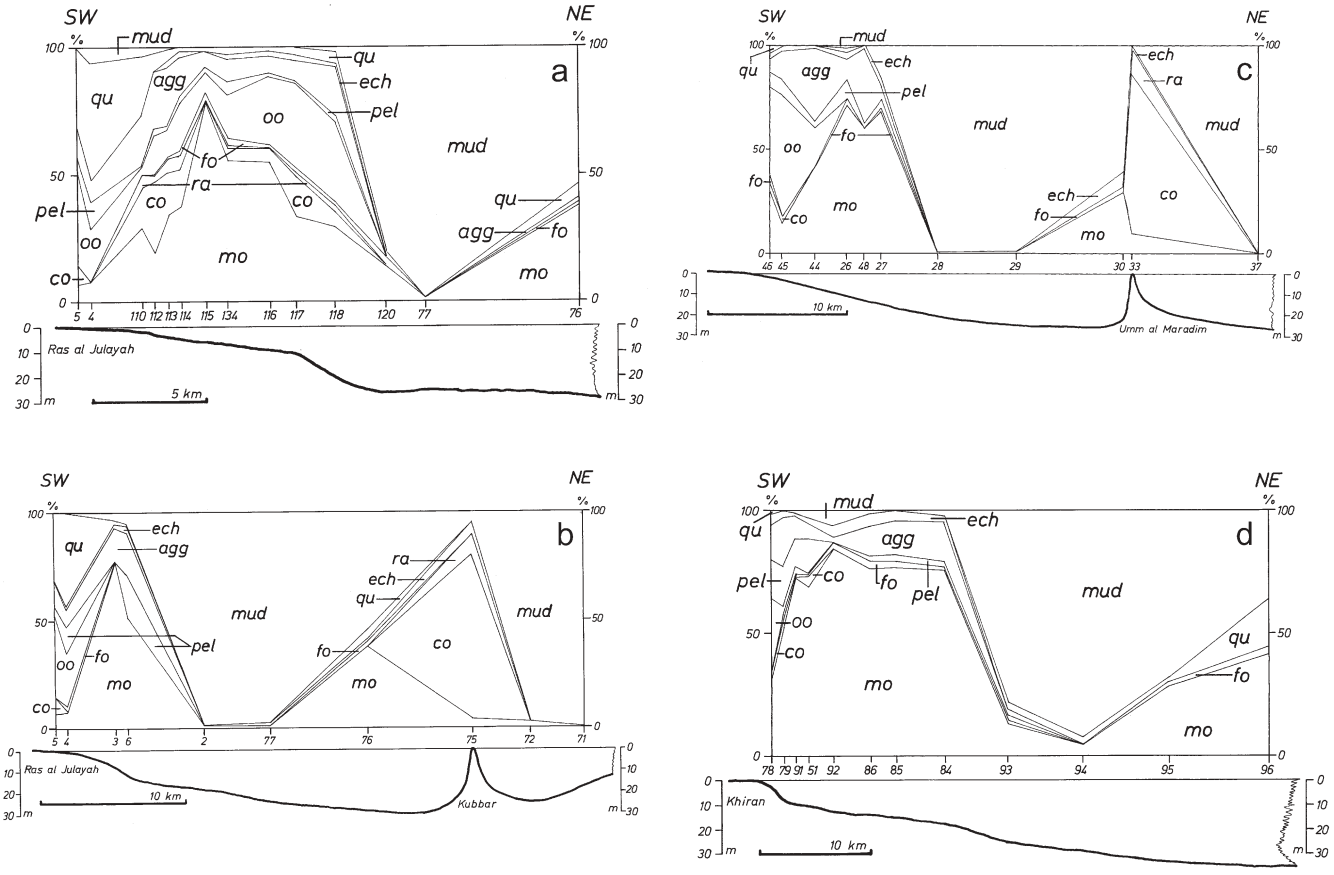

Fig. 7 Four cross sections (a–d) through study area showing distribution of constituent grain types and fine-grained carbonate <0.125 μm. *qu* quartz, *oo* ooid, *co* coral, *fo* foram, *mo* mollusk, *agg* aggregate grain, *pel* pellets, *ra* red alga, *ech* echinoderm. For practical reasons, we shifted Dunham's upper grain-size limit for mud from 20 to 125 μm

gregate grains is 14.6%. Apart from non-skeletal grains, mollusks are common. Their abundance is quite variable, between 5–48%, averaging 25.4%. Fragments of corals and coralline algae occur with average abundances around 5%. Mud content averages 0.9%. The amount of insoluble residue averages 10.4% and is of both fine-grained quartz and clay mineral origin. Aragonite is the dominant carbonate mineralogy with values of 92–98% relative abundance.

In addition, an *aggregate grain packstone to grainstone sub-facies* is mapped out in places where this grain type exhibits abundances exceeding 20% (Fig. 11). There are three areas in which this situation occurs all of which are in the inner and mid ramp and between 5–15 m water depth (off Ras Al-Julayah; between Ras Al-Julayah and Ras Al-Zour; south of Ras Al-Zour and off Al-Khiran). Even though this facies could not be delineated by statistical means we decided to separate it for practical reasons. Aggregate grains, especially the common ooid grapestones, are easily recognized and give this sub-facies a characteristic appearance (Fig. 4e, f).

Mollusk packstone to grainstone.- This facies covers a 5–15 km wide area of the mid ramp environment (Fig. 11). Water depths typically range from 7.5–17 m, however, a small number of samples falls outside this range (Table 5). The average depth of samples of this facies is 11 m. The most common constituent particles are mollusk shells (Fig. 5a, b). Their abundance ranges from 28.9–85.5% with an average of 61%. Non-skeletal grains reach an average abundance of 21%. Of these, aggregate grains are most common (average 12%). Locally, elevated abundances of echinoderm fragments are observed. Benthic foraminifera reach their highest abundances in this facies, although in general this grain type was found to be conspicuously rare in the study area. Amounts of mud are variable and range from 0–42.8% with an average 7.4%. Insoluble residue averages 11.8% and is mostly due to the presence of clay minerals as the average abundance of quartz grains is <1.8%. Carbonate mineralogy exhibits high variability as seen in the wide ranges of relative abundances of aragonite (28–97%), high-Mg-calcite (2–19%), and low-Mg-calcite (1–51%). On average, aragonite is most common.

Mollusk-marl wackestone.- This facies covers the outer ramp areas in water depths commonly exceeding 17 m (Fig. 11). The average depth for samples of this facies is 22.5 m (Table 6). Mud is most common in this facies ranging from 36–99% with an average of 79%. Most of this mud is made up of clay minerals since insoluble residue in this facies averages 55.7% and only 2.5%

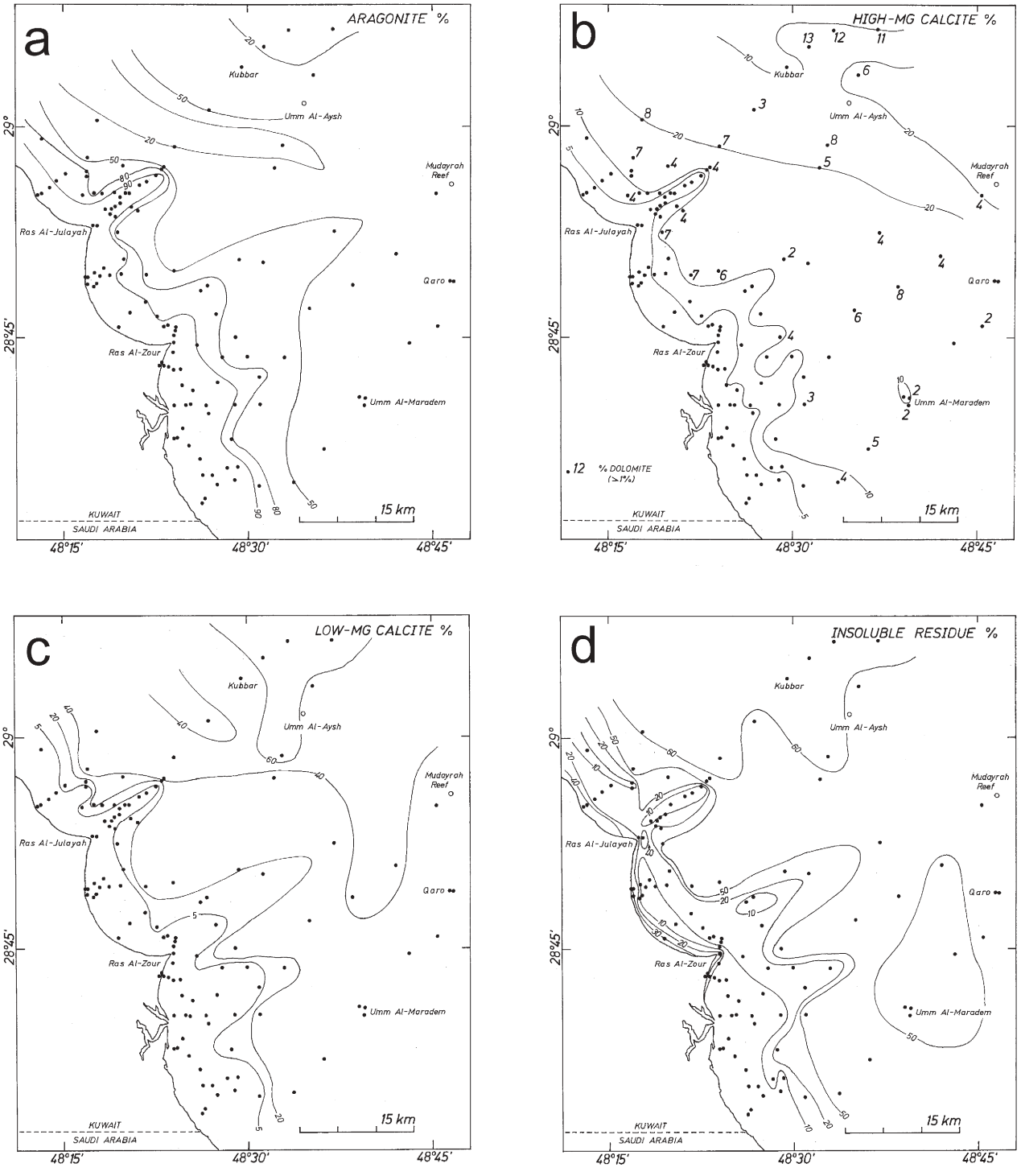

Fig. 8 a Map of aragonite distribution. **b** Map of high-Mg-calcite and dolomite (*large numbers*) distribution. **c** Map of low-Mg-calcite distribution. **d** Map of insoluble residue distribution. Numbers are in %

quartz is present on average. Mollusk shells are the most common grain constituents (Fig. 5c, d). Their abundance ranges from 0.2–41% and averages 14.9%. Like in the mollusk packstone to grainstone facies, echinoderm fragments may be common locally. Carbonate mineralogy is highly variable with aragonite (42.3%) and low-Mg-calcite (37.9%) being most common on average. High-Mg-calcite abundance averages 14.3%. Dolomite may be present with up to 11.5% relative abundance locally.

Coralgal grainstone.- This facies is common on and around the isolated outer ramp reefs and reef islands as well as on small inner ramp patch reefs (Fig. 11). Water depths of investigated samples range from 0–10.5 m (Table 7). With average abundances of 62.1 and 10.7%

Table 1 Correlation matrix of compositional, textural, and mineralogical data (upper value is r; statistically significant correlation at p<0.05)

	Mollusk	Coral	Redalga	Foram	Ooid	Pellet	Aggregate	Echino	Quartz	Mud	Insoluble Res.	Depth (m)	LMC	ARA	DOL	HMC
Mollusk	1 p<.000															
Coral	−.26942 p<.002	1 p<.000														
Redalga	−.21721 p<.013	.87919 p<0.000	1 p<.000													
Foram	.35902 p<0.000	−.22308 p<.011	−.21615 p<.014	1 p<.000												
Ooid	−.31745 p<0.000	−.05887 p<.506	−.07929 p<.370	−.10795 p<.222	1 p<.000											
Pellet	.08635 p<.329	−.17671 p<.044	−.18354 p<.037	−.04988 p<.573	.34949 p<0.000	1 p<.000										
Aggregate	.23142 p<.008	−.05832 p<.510	−.06835 p<.440	−.22348 p<.011	.13344 p<.130	.21389 p<.015	1 p<.000									
Echino	.33816 p<0.000	.01470 p<.868	.14206 p<.107	.33296 p<0.000	−.21167 p<.016	−.03499 p<.693	−.10163 p<.250	1 p<.000								
Quartz	−.22517 p<.010	−.08485 p<.337	−.07993 p<.366	−.08169 p<.355	.16696 p<.058	.01562 p<.860	.04305 p<.627	−.20578 p<.019	1 p<.000							
Mud	−.48844 p<0.000	−.23772 p<.006	−.22473 p<.010	−.05476 p<.536	−.38282 p<0.000	−.40264 p<0.000	−.53975 p<0.000	−.14387 p<.102	−.17659 p<.044	1 p<.000						
Insoluble Res.	−.52375 p<0.000	−.27422 p<.002	−.25730 p<.003	.01915 p<.829	−.31317 p<0.000	−.41315 p<0.000	−.48141 p<0.000	−.16506 p<.061	.27263 p<.002	.85459 p<0.000	1 p<.000					
Depth	.05129 p<.562	−.37825 p<0.000	−.31867 p<0.000	.17053 p<.052	−.51687 p<0.000	−.45616 p<0.000	−.40656 p<0.000	−.02793 p<.752	−.16194 p<.066	.69091 p<0.000	.64364 p<0.000	1 p<.000				
LMC	−.43075 p<0.000	−.21281 p<.015	−.19665 p<.025	.03765 p<.671	−.35673 p<0.000	−.41410 p<0.000	−.49274 p<0.000	−.10916 p<.216	−.11901 p<.177	.89384 p<.000	.85684 p<0.000	.68553 p<0.000	1 p<.000			
ARA	.39118 p<0.000	.19092 p<.030	.16849 p<.055	−.08030 p<.364	.41860 p<0.000	.46805 p<0.000	.51169 p<0.000	.08350 p<.345	.11770 p<.182	−.89572 p<.000	−.86535 p<0.000	−.72893 p<0.000	−.98572 p<.000	1 p<.000		
DOL	−.48750 p<0.000	−.19531 p<.026	−.19245 p<.028	−.04989 p<.573	−.31133 p<0.000	−.36988 p<0.000	−.36492 p<0.000	−.13894 p<.115	−.00077 p<.993	.82661 p<0.000	.84540 p<0.000	.55976 p<0.000	.91076 p<.000	−.91372 p<.000	1 p<.000	
HMC	−.10987 p<.213	−.06859 p<.438	−.02327 p<.793	.25551 p<.003	−.54735 p<0.000	−.55447 p<0.000	−.49916 p<0.000	.04604 p<.603	−.13805 p<.117	.68502 p<0.000	.65999 p<0.000	.74442 p<0.000	.70217 p<0.000	−.80733 p<0.000	.62516 p<0.000	1 p<.000

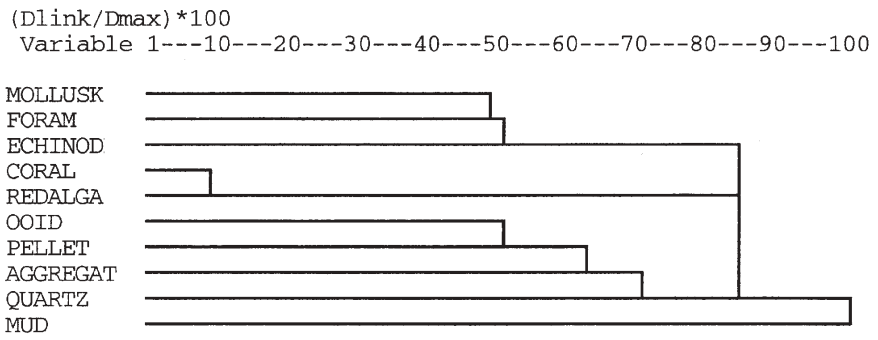

Fig. 9 Results of an r-mode cluster analysis of constituent grains and fine-grained sediment ("mud") using unweighted pair-group average, Euclidean distances. (This algorithm produced the most meaningful dendrogram entities)

Table 2 Results of a factor analysis using composition and textural data showing four factor loadings, which account for a variance of 73.5%

	Factor 1	Factor 2	Factor 3	Factor 4
Mollusk	–0.527896	+0.568473	–0.460075	–0.208406
Coral	–0.196021	–0.885393	–0.308415	+0.074471
Algae	–0.198297	–0.857272	–0.375887	+0.104140
Forams	–0.004524	+0.523845	–0.427851	+0.520524
Ooids	–0.341784	–0.101589	+0.642250	+0.453332
Peloids	–0.507725	+0.211949	+0.407150	+0.190290
Aggregate	–0.612608	+0.061778	+0.280042	–0.512766
Echinoderm	–0.190785	+0.190348	–0.656250	+0.316306
Quartz	+0.098855	–0.054708	+0.502134	+0.315104
Mud	+0.943304	+0.047957	–0.060370	–0.151593
Insoluble Res.	+0.952631	+0.069424	+0.105069	+0.039063
Variance	0.268166	0.201983	0.180482	0.096297

respectively, fragments of corals and coralline algae are most common. Mollusks are common locally and reach an average abundance of 14.5%. Aggregate grains reach an average abundance of 5.5%. Mud content is very low with an average of <1%. Insoluble residue averages 6.2% and is mostly clay minerals as quartz grains are very rare. Carbonate mineralogy is clearly dominated by aragonite and high-Mg-calcite. On the shores of the reef islands of Kubbar, Qaro, and Um Al-Maradem, coralgal sands are well-cemented to form local occurrences of intertidal beachrock (Fig. 5e, f). The most common cement is the aragonite needle type, which occurs in form of isopachous crusts around constituent grains, confirming an early marine-phreatic diagenetic environment.

Stable isotopes

Stable isotopes of carbon and oxygen were measured for bulk carbonate-rich samples of the ooid-skeletal grainstone, the mollusk packstone to grainstone, the coralgal grainstone facies, and selected end members such as corals, mollusks, and others (Fig. 12). In bulk samples, $\delta^{13}C$ ranges from +0.5 to +4.2‰ PDB and $\delta^{18}O$ from –1.2 to +1.0‰ PDB. Individual facies have narrower ranges of values, and three herds may be seen in Fig. 12. Correlation analysis shows that carbon and oxygen isotopes are highly correlated with carbonate mineralogy (Table 8) and hence with abundances of skeletal types. It is likely that the significantly lighter carbon and oxygen values for the coralgal facies samples as compared to those of the other two facies are related to biological fractionation within the corals. The heavier carbon values of the ooid-skeletal facies samples as compared to those of the mollusk facies may be explained by the differences in water depths and hence illumination. Primary production is higher in the shallower water of the ooid-skeletal facies and lower in the deeper water of the mollusk facies. Consequently, more of the lighter ^{12}C is removed from the system in shallower water leading to heavier values in the precipitated carbonates. Indeed, the correlation between carbon isotopes and water depth is statistically significant ($r = -0.478$, $p<0.0001$).

For comparison, Weber (1967) and Weber and Woodhead (1969) measured ranges in $\delta^{13}C$ of bulk carbonate sediments of +1.6 to +4.5‰ and +0.75 to +3.2‰ on the Bermuda platform and on Heron Reef in the Great Barrier Reef, respectively. $\delta^{18}O$ from these settings ranged from –0.6 to +0.4‰ in Bermuda and from –2.1 to –0.4‰ on Heron Reef. In Land's (1989) compilation of isotope data from shallow marine carbonate sediments, values ranged from about –3.5 to +5‰ for $\delta^{13}C$ and from –3.5 to +2‰ for $\delta^{18}O$. Interestingly, the isotopic composition of constituent carbonate sediment particles such as corals, algae, mollusks, foraminifera, and others also exhibit large variation in $\delta^{13}C$ and $\delta^{18}O$. Even so, isotopes of bulk samples from ancient—largely Cretaceous—shallow water carbonate settings of ramps and platforms

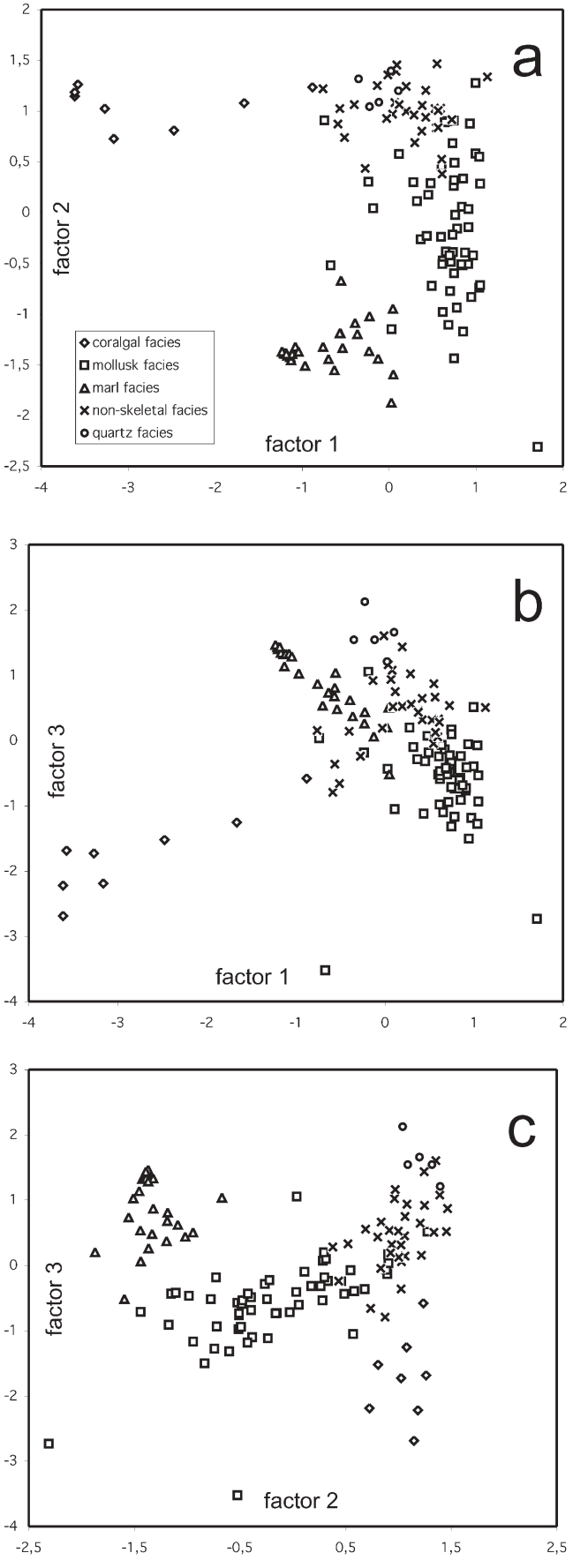

have been used repeatedly for carbon isotope stratigraphy (Jenkyns 1995; Vahrenkamp 1996; Vallardes et al. 1996; Drzewiecki and Simo 1997; Ferreri et al. 1997; Mutti et al. 1997; Grötsch et al. 1998; Wissler et al. 2003). In these studies, $\delta^{13}C$ ranges from about −1 to +5‰ and individual stratigraphic sections show an absolute range from about 2 to 4‰. Vallardes et al. (1996) reported a total range of 8‰ for $\delta^{13}C$. Recently, Cozzi et al. (2004) used $\delta^{13}C$ profiles of bulk samples in order to correlate stratigraphically within a Proterozoic ramp.

According to our study and the above-mentioned studies of C- and O-isotopes in modern shallow water carbonate sediments (Weber 1967; Weber and Woodhead 1969; Land 1989), the reported ranges in $\delta^{13}C$ and $\delta^{18}O$ from fossil ramp and platform sections could easily be explained by lateral facies shifts or just by slight changes in taxonomic composition within individual carbonate-producing organism groups. Additional effects which may influence carbonate isotopic composition include depletion in ^{13}C of carbonate bank waters due to the decomposition of organic matter (Patterson and Walter 1994), changes in $\delta^{18}O$ during burial diagenesis, and possible meteoric diagenesis (Immenhauser et al. 2003). Therefore, results of bulk analyses of carbon and oxygen isotopes of shallow water carbonate settings should only be used very carefully for stratigraphic and paleo-environmental interpretations.

Discussion

Depositional environment and comparison with other modern ramp systems

The distribution of sedimentary facies on the southern Kuwait carbonate ramp is interpreted to be largely controlled by water depth, i.e., by depositional energy (Fig. 13). Facies boundaries run more or less parallel to bathymetric contours and the abundances of the great majority of constituent grains, of the fine grain-size fractions, and mineralogy and isotope geochemistry exhibit statistically significant correlations with water depth. Exceptions to the latter rule are fragments of mollusks and echinoderms. Mollusk fragments are the most abundant skeletal grains in the entire study area and they are common in all water depths. Echinoderms appear to be most common in intermediate depths. Non-skeletal grain accumulation is favored in shallow depths with ooids being most common and aggregate grains extending into deeper water as seen in their relative abundance in the inner and mid ramp area.

A comparison of our data with modern sedimentary facies of the southern Arabian-Persian Gulf (Houbolt 1957; Wagner and Van der Togt 1973; Purser 1974) re-

Fig. 10 Results of a factor analysis (**a** – **c**) showing scatterplots of 130 factor scores (factors 1–3). Note that samples from individual facies form separate herds

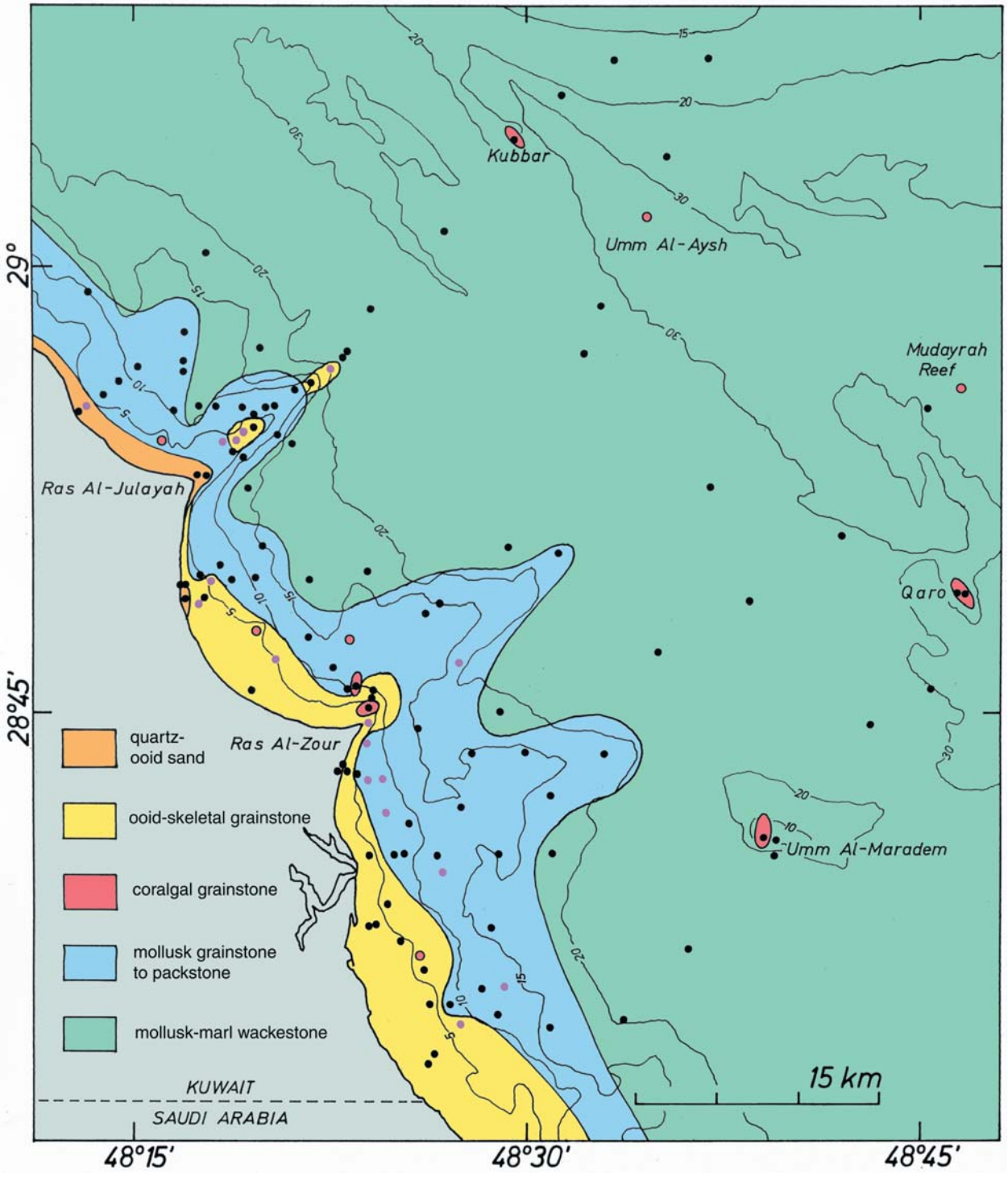

Fig. 11 Facies map of the study area. *Dots* indicate sample locations. *Pink dots* mark the aggregate grainstone to packstone sub-facies, in which aggregate grain abundances exceed 20%. Depth contours are in meters

veals a number of similarities but also important differences. As in our study area, there are mollusk (bivalve and gastropod), coralgal, non-skeletal (ooid, aggregate), marl, and quartz-rich facies. Unlike the northern area, however, there is a foraminiferal facies. It remains enigmatic why foraminifera are so rare in the northern Gulf as compared to the southern Gulf areas. The existence of barrier islands and shoals is one of the major differences between the southern and northern realms of the Arabian-Persian Gulf in general (Lomando 1998, 1999). In the south, barriers modify the pure control of depositional energy on facies distribution in that muddy sediment is

Table 3 Composition, texture, and mineralogy of quartz-ooid sands

Sample	Mollusk	Coral	Red Algae	Foram	Ooid	Peloid	Aggregates	Echinoderms	Unknown	Quartz	"Mud"	Insoluble Res.	Depth (m)
K 004	7.5	0.5	0	1	24	11	7.5	1.5	1.5	45.5	0.1	46.9	0
K 005	6.8	7.8	0	0	37.8	3.9	10.7	1	0	32	0.1	19.0	0
K 011	20.9	2	0	0	21.8	5	9.9	0	2.5	37.2	0.7	43.2	2.9
K 126	12.5	3	0.5	0.5	2.5	2	33.9	0.5	0.5	43.9	0.2	57.1	3.3
K 127	9	0	0	1	20.4	4.5	3	0	0	61.8	0.4	58.3	0
Mean	11.34	2.66	0.10	0.50	21.30	5.28	13.00	0.60	0.90	44.08	0.30	44.90	1.24
Min	6.8	0	0	0	2.5	2	3	0	0	32	0.1	19	0
Max	20.9	7.8	0.5	1	37.8	11	33.9	1.5	2.5	61.8	0.7	58.3	3.3

Table 4 Composition, texture, and mineralogy of ooid-skeletal grainstones

Sample	Mollusk	Coral	Red Algae	Foram	Ooid	Peloid	Aggregates	Echinoderms	Unknown	Quartz	"Mud"	Insoluble Res.	Depth (m)
K 010	21.3	1	1	1	44.7	14.4	11.9	2	2	0	0.7	6.0	4.3
K 012	32.4	1.5	0	3	35.9	6	13.4	1.5	2	4	0.4	5.5	4.5
K 013	47.7	2.5	0.5	0.5	9.4	5.5	29.3	1	2.5	0.5	0.6	6.1	7.6
K 014	31.6	2	0.5	0.5	31.6	7.9	20.7	1.5	1	1.5	1.4	12.0	5.0
K 019	31	1	0	1	11.9	31	16.2	1.4	1.5	0.5	4.5	6.5	4.5
K 020	28.5	1.8	0	0.9	26.7	19.8	4.6	2.3	0.9	6.5	8.1	10.0	2.8
K 021	20.1	1	1	2.6	27.3	22.1	4.1	3.1	1.6	15.4	0.7	17.3	0.0
K 022	40.4	3.3	1.3	0	31.8	11.2	8.6	0.7	0	2	0.7	5.2	5.5
K 023	19.9	5	0	1.5	36.4	12	17.4	3.5	1	3	0.3	7.9	1.6
K 024	29.9	5.5	0	4	38.4	9.5	5.5	1.5	2	3.5	0.4	9.0	1.0
K 025	17.9	6.5	0	1	54.8	7.5	8	1	2	1	0.3	4.1	6.3
K 041	4.9	0.8	0	0.8	82.6	8.1	0.8	0.8	0.8	0	0.3	7.8	5.5
K 042	14.5	1.5	0	2.5	57.9	5	12.5	0	6	0	0.1	7.1	4.3
K 044	41.3	0	0	0	18	3	35.4	2	0	0	0.4	6.6	7.5
K 045	13.4	3.5	0	0	58.8	7.5	13.9	1.5	1	0	0.4	6.2	3.5
K 046	27.8	4	0	1.7	46	6.8	5.7	2.3	0.6	5.1	0.1	8.8	2.0
K 055	12.2	2.6	2.1	1.6	41.4	14.8	2.6	3.1	1.6	16.8	1.5	22.2	3.5
K 056	13.5	4.5	1.5	0.5	12.5	2.5	39.4	2	0.5	23	0.2	14.2	1.5
K 057	16	21	4	2	21	1.5	25	2	1.5	6	0	10.6	1.2
K 059	14.5	8.5	1	0.5	49.9	9.5	7	1.5	0.5	7	0.2	11.6	1.0
K 060	29.4	8	3.5	0	36.9	3	14	2	0	3	0.2	14.2	2.0
K 063	22.6	5.1	0	2	39.8	4	24.1	2	0	0	0.3	7.1	5.7
K 064	14.5	3	0.5	1.5	33	6.5	8.5	1.5	1.5	29.5	0.1	29.6	2.8
K 078	31.7	1.5	0.5	0	29.3	15.4	13.4	4.5	1.5	1.5	0.8	7.6	2.5
K 105	28.8	2	0	0	29.3	15.9	20.9	0	1	1.5	0.6	6	6.0
K 106	33.2	0.9	1.9	1.9	26.1	12.3	11.9	0.5	1.4	4.7	5.1	10.7	3.0
K 107	19.4	0.5	0	0.5	45.3	12	5.5	0	2	13.9	0.4	18.9	1.5
K 112	19	28.5	2	0.5	16.5	2.5	22.5	0	0.5	8	0	16.6	1.8
K 113	34.4	17	5.5	1	9.5	1.5	23.4	2.5	0	5	0.2	11.6	4.6
K 114	37.5	15	5.5	1.5	18	3.5	14.5	2	0	2.5	0	10.9	4.8
K 117	33.5	16	2	2	32.5	1	7.5	2.5	0	3	0	8.5	10.5
K 118	29.5	6	2.5	1.5	31.5	2.5	20	1	1	4.5	0.1	7.6	21.0
Mean	25.38	5.66	1.15	1.19	33.90	8.93	14.63	1.66	1.18	5.40	0.91	10.44	4.35
Min	4.90	0.00	0.00	0.00	9.40	1.00	0.80	0.00	0.00	0.00	0.00	4.10	0.00
Max	47.70	28.50	5.50	2.60	82.60	31.00	39.40	4.50	2.50	29.50	8.10	29.60	21.00

deposited behind these features. Farther offshore, the abundance of fines increases with increasing water depth just as in the area of our study. Another difference is the depth of transition between mud-supported and grain-supported textures. In the south it is situated in about 36 m of water whereas in the north it lies at ca. 17 m. A plausible reason for this difference is the fact that the predominating Shamal wind has more fetch in the south and that the southern Gulf is deeper allowing for a deeper wave base.

Comparisons with the modern tropical to subtropical humid ramp examples of Campeche Bank, Yucatan (Cann 1962; Logan et al. 1969; Lomando 1999), and the western Florida shelf (Gould and Stewart 1955) farther afield reveal significant differences. In these modern distally-steepened ramp examples, inner and mid ramp areas are characterized by mollusk-dominated facies and shoreline systems ranging from simple shorelines to barrier island-lagoon complexes. In the case of western Florida clastics can dominate in the inner ramp realm. Outer ramp areas, however, are covered irregularly by coralline algae, relict ooids, and in the case of Campeche Bank, isolated coral reefs are found. An additional comparison with an arid, homoclinal ramp would be desirable, however, the data available on the most prominent example, the Gulf of Carpentaria of northern Australia, are only limited. Jones (1987) described surface sediments of parts of Gulf of Carpentaria and noted quartz, mollusks, foraminifera, echinoderms, ostracods, and ooids as major constituents of surface sediments. Even so, there are no detailed data

Table 5 Composition, texture, and mineralogy of mollusk packstones to grainstones

Sample	Mollusk	Coral	Red Algae	Foram	Ooid	Peloid	Aggregates	Echinoderms	Unknown	Quartz	"Mud"	Insoluble Res.	Depth (m)
K 001	72.8	0	0	2.8	0	7	3.3	1.9	4.2	1.9	6.1	8.8	10.0
K 003	74.4	0	0	3.5	0	0	14.7	1.5	1.4	1.4	3.1	18.4	13.5
K 006	50.5	1	0	0	0.5	19.9	19.4	2.4	1.9	1	2.8	8.7	8.0
K 007	63.6	1	0	1	0	6.4	9.4	3.5	2	2	11.3	12.5	9.5
K 008	55	0.9	0	0.9	0	15.9	12.6	2.8	3.3	1.8	6.6	8.2	10.2
K 009	53.2	0	0	2	7.5	13.4	15.4	4	3.5	0.5	0.5	7.2	6.3
K 015	40.1	17.7	1.7	1.3	2.1	7.6	12.7	0.4	0.8	0	15.5	10.5	8.5
K 017	60.7	0.5	0	0.5	0	3	31.1	2	1	0	1.3	7.1	8.2
K 018	37.6	2	0	1	11.2	24.9	19.5	0	1.5	0	2.3	7.3	6.4
K 026	73.2	0	0	1.5	0	7.9	10.3	3.4	0.5	1.5	1.8	7.4	11.0
K 027	68.1	1.3	0	1.9	0	4.5	5.8	2.6	7	0.6	8.3	16.0	15.0
K 043	70.2	0	0	0.4	0	4.6	6.2	6.2	0.5	0.5	11.3	12.6	13.3
K 047	70.5	0	0	0.5	4.2	6	12.2	4.2	0	0	2.5	5.4	8.5
K 048	59.5	0	0	0	0	1.8	36.7	1.8	0	0	1.2	8.0	13.5
K 049	50.4	0	0	0.8	2.4	3.2	15.2	3.5	0.8	0.8	23.1	20.6	16.5
K 050	68	0	0	0	0	0	28.7	0.7	0	2.2	0.4	6.0	12.5
K 051	68.4	4	0	0.5	2	14.4	5.9	2	1.5	0.5	0.9	6.7	10.0
K 052	50.5	3	0	0	2	7.4	32.7	1.5	1	1	0.9	7.7	9.5
K 053	50.8	0	0	0	3.7	12.2	25.4	0.5	0.5	0.5	1.6	5.7	7.5
K 054	51.2	2.5	0	0	5	6.2	32	1.2	0.6	0.6	0.8	5.7	6.8
K 061	46.3	0.6	0	1.2	0	1.8	0.6	5.5	0.6	0.6	42.8	17.0	14.0
K 062	71.2	0	0.5	0.9	0	1.9	12.3	5.7	0.9	0.9	5.7	13.1	13.2
K 065	62.8	0.5	0.5	2.5	0	3	24.6	1.5	1.4	0	3.5	14.1	16.2
K 079	52.2	3.5	0	1.5	2.5	15.9	19.4	3	0	1.5	0.6	6.9	8.3
K 080	78.5	2.2	0	1.1	0	3.3	4.4	6.6	1.1	1.1	1.6	9.3	10.7
K 081	71.2	2.7	0	2.1	0	2.1	8.7	4.4	0.6	4.9	3.2	8.4	16.2
K 083	77.3	0	0	2.6	0	0.7	8	6.7	2.1	0.7	1.9	8.4	16.5
K 084	75.4	0	0	1.3	0	2	16.1	2.6	1.3	0	1.5	12.0	17.5
K 085	76.4	0	0	2.1	0	2.8	13.2	4.9	0.7	0	0	12.0	15.3
K 086	76	0	0	3.3	0	2.3	11.2	5.1	0	0.5	6.7	11.7	14.2
K 087	45.3	0	0	5.9	2	5.6	0	4.3	0.7	2.1	34.3	16.0	17.3
K 091	72.4	0	0	1.5	0.5	10.9	8.9	1.5	3	0.5	0.8	5.6	10.0
K 092	84.6	0	0	2.4	0	0	1.9	4.3	1.9	0	4.8	9.7	18.0
K 098	65.4	0	0	3.9	0	0.8	5.8	1.2	0	0.8	22.2	20.5	23.0
K 099	85.5	0	0	2.5	0	0	9.9	1	0	0	1.2	4.6	15.0
K 100	76.9	0	0	2.5	3.5	3.9	7.9	2	2	0	1.4	5.5	12.2
K 103	52.5	0	0	1.4	0	19.2	15.9	1.9	0	2.8	6.2	10.8	12.0
K 104	50.8	0	0	1.6	0	16.7	2.8	3.6	1.6	1.6	20.7	10	9.0
K 109	42.4	0	0	2.7	0	10.9	0.3	4.1	1	6.8	31.6	23.8	12.8
K 110	28.9	16.5	4.5	1	3.5	0.5	18.5	0.5	1.5	24.5	0.1	24.9	2.3
K 111	47.4	9	2.5	0	4	1.5	27.9	5.5	0	2	0.3	8.9	2.9
K 115	76.8	2.5	0	3	8	1.5	6	0.5	0	1.5	0.2	5.1	6.0
K 116	54.5	5	0	1.5	26.5	1	6.5	2	1.5	1.5	0	7.1	8.0
K 122	53.4	0	0	9.9	0	4.2	0.5	12.6	1.1	1.6	16.8	63.5	14.5
K 123	68.6	0	0	3.4	0	2.6	5.1	1.7	0.9	3.4	14.3	16.6	12.0
K 124	62	1.3	0	3.1	0	2.6	13.6	1.3	1.3	2.6	12.1	13.8	9.0
K 125	62.3	2	0	0.5	13.8	6.9	6.9	1	2	3.5	1.1	7.2	6.0
K 128	63.6	0	0	4.5	0	5	10.5	3.6	1.4	2.3	9.1	12	10.4
K 130	53.1	0	0	5.3	0	2.7	8.3	4.2	1.1	1.1	24.1	22.8	10.0
K 131	49	16	9.2	1	0	1	3.9	16	1.5	0.5	3	5.8	7.5
K 132	69.1	3.5	3	2.5	5	4.5	6.5	3.5	1	1	0.6	6.6	7.5
K 133	52.4	3.5	0	2.5	18	12.5	5	1	0	5	0.2	7.7	5.2
K 134	55.5	4	1.5	2.5	17	5	9.5	1.5	0	3.5	0.1	7.8	7.0
K 135	50.3	6.2	0	1.4	23	4.3	8.1	0.5	0	1.9	4.2	8.4	10.4
K 136	55.2	0	0	4.7	1.8	5.8	0	2.2	0.7	2.2	27.4	21.8	14.0
Mean	60.98	2.05	0.43	1.97	3.09	6.03	11.96	3.16	1.18	1.81	7.39	11.82	11.07
Min	28.90	0.00	0.00	0.00	0.00	0.00	0.00	0.00	0.00	0.00	0.00	4.60	2.30
Max	85.50	17.70	9.20	9.90	26.50	24.90	36.70	16.00	7.00	24.50	42.80	63.50	23.00

given, and a comprehensive sediment study of this important example of an arid epicontinental sea would indeed be desirable. It would furthermore be useful to extend the area studied here to the Saudi Arabian offshore area to the south in order to cover the entire Arabian-Persian Gulf ramp and to get a comprehensive picture of facies distribution and, in particular, facies transitions.

Comparison with ramp systems in the fossil record

Carbonate ramps with shoreline and offshore ooid shoals—comparable to our modern Kuwait example—occur throughout the Phanerozoic (Burchette and Wright 1992; Wright and Burchette 1998). Wilson (1975) recognized that the Early Carboniferous (Mississippian) was a period of abundant and widespread oolite deposition in North America and in many cases the oolites form significant oil and gas reservoirs (Handford 1988) as, e.g., in

Table 6 Composition, texture, and mineralogy of mollusk-marl wackestones

Sample	Mollusk	Coral	Red Algae	Foram	Ooid	Peloid	Aggregates	Echinoderms	Unknown	Quartz	"Mud"	Insoluble Res.	Depth (m)
K 002	0.3	0	0	0.1	0	0.1	0	0.7	0	0	98.8	64.5	18.0
K 028	0.5	0	0	0.1	0	0.1	0	0.5	0	0	98.7	66.2	20.5
K 029	1.2	0	0	0.2	0	0	0	0.4	0	0.2	97.9	65.9	25.0
K 030	29.9	0	0	3.1	0	1.8	0	6.7	2	1.1	55.3	39.7	22.0
K 031	15.1	0	0	0.9	0	0.3	0	3.6	0.8	0.3	78.9	48.0	16.0
K 066	30.8	0	0	1.4	0	0.4	0.2	2.7	0.6	4.9	58.9	46.2	22.5
K 067	29.2	0	0	1.6	0	0.2	2	1.2	0.4	5.9	59.5	57.7	25.0
K 068	1.6	0	0	0.4	0	0	0	0.8	0	0	97.3	65.1	31.5
K 069	23.8	0	0	6.1	0	0	1	0.8	0	0	68.3	55.5	23.5
K 070	0.6	0	0	0.1	0	0	0	0.5	0	0	98.8	65.1	17.0
K 071	0.2	0	0	0	0	0	0	0.4	0	0	99.3	65.1	17.2
K 072	0.5	0	0	0.1	0	0	0.1	2.3	0	0	96.9	63.5	25.0
K 076	38	0	0	1.7	0	0.2	2.5	1	1.2	4.4	51	49.5	28.0
K 077	1.1	0	0	0.2	0	0	0	0.9	0	0	97.7	69.0	25.0
K 082	22.2	0	0	1.2	0	0.6	0.4	3	0	1.6	71	50.5	17.5
K 088	2.4	0	0	0.4	0	0.3	0	0.7	0.1	0.2	96	58.3	19.7
K 093	13.1	0	0	1.1	0	0	1.3	1.8	0	2.8	79.9	56.1	25.7
K 094	4.5	0	0	0.4	0	0	0.2	0.6	0	2.3	91.9	62.4	28.5
K 095	28.8	0	0	1.2	0	0	0.3	0.2	0.2	1.8	67.5	44.6	33.7
K 096	41	0	0	3.5	0	0	0	0.3	0.3	18.9	35.9	57.6	35.0
K 097	25.8	0	0	0.5	0	0	2.6	0.7	0.7	17.3	52.6	58.9	28.8
K 101	4.6	0	0.1	1.1	0	0	0	1.7	0.1	0	92.4	55.4	15.5
K 102	1.1	0	0	0.3	0	0	0	0.3	0	0.1	98.3	63	19.0
K 108	3.9	0	0	0.6	0	0.7	0	0.7	0.1	0.8	93.4	52.9	15.0
K 120	14.2	0	0	2.3	0	0	0.1	1.5	0.1	0.3	81.4	53.9	26.0
K 121	31.4	0	0	2.9	0	1	0	3.3	0.2	2.5	58.7	43.8	16.8
K 129	28.9	0	0	2.5	0	1.5	0.4	2.6	0.2	1.7	62.2	38.5	13.0
K 137	23.1	0	0.2	1.1	0.2	1.7	0.2	1.7	0.2	2	70	43.6	18.4
Mean	14.92	0.00	0.00	1.25	0.00	0.32	0.40	1.49	0.26	2.47	78.88	55.73	22.46
Min	0.20	0.00	0.00	0.00	0.00	0.00	0.00	0.20	0.00	0.00	35.90	38.50	13.00
Max	41.00	0.00	0.20	3.50	0.20	1.80	2.60	6.70	1.20	18.90	99.30	69.00	35.00

Samples K 037 and K038 were not used here as there is not enough sample material

Table 7 Composition, texture, and mineralogy of coralgal grainstones

Sample	Mollusk	Coral	Red algae	Foram	Ooid	Peloid	Aggregates	Echinoderms	Unknown	Quartz	"Mud"	Insoluble Res.	Depth (m)
K 016	27.4	40.8	8.5	0.5	1	6	12.9	1.5	1	0	0.4	15.6	7.8
K 033	9.8	76.8	12.2	0	0	0	1.2	0	0	0	0	3.2	0.0
K 035	15.1	68.1	7	1.1	0	0	6.5	1.6	0.5	0	0	3.1	0.0
K 039	21.5	56	19	0	0	0	0	3.5	0	0	0.1	3.1	10.5
K 040	15	67.5	15.5	0	0	0	0	2	0	0	0	2.9	0.0
K 058	11	35.9	3.5	1	13	7	23	2.5	1.5	1.5	0.2	8.2	1.0
K 074	12	76.4	10	0	0	0	0	1.5	0	0	0.1	3.1	0.0
K 075	3.8	75.5	9.5	0	0	0	0	5.7	0.5	0	5	10.2	0.0
Mean	14.45	62.13	10.65	0.33	1.75	1.63	5.45	2.29	0.44	0.19	0.73	6.18	2.41
Min	3.8	35.9	3.5	0	0	0	0	0	0	0	0	2.9	0
Max	27.4	76.8	15.5	1.1	13	7	23	5.7	1.5	1.5	5	15.6	10.5

the subsurface of the Illinois Basin. Some of these paleoshoal trends contain oolitic carbonates that transition offshore to mixed carbonate-siliciclastic sediments (Manley et al. 1993). Mississippian cycles from the Golconda Group (Harris and Freuenfelter 1993; Manley et al. 1993) are an exceptionally good analogue to the northern Arabian-Persian Gulf in both facies distribution and scale. The paleo-Michigan River delta, northwest of the main carbonate ramp trend, provided significant siliciclastics to the basin. Oolitic shoals developed approximately 80–100 km from the delta front and continue for several hundred kilometers. Offshore areas are dominated by siliciclastic-rich carbonate muds (marls) to calcareous shales punctuated by sporadic bioclastic shoal grainstones analogous to the outer ramp reefs and shoals of southern Kuwait.

What we observe in the offshore of southern Kuwait is an expected progression of facies belts for inner to mid to outer ramp systems. Modifications to the expected scheme include the sub-parallel nature of facies trends and the discontinuous nature of facies continuity along strike. Etterson (1993) reviewed Mississippian depositional trends across central North America and concluded that of all the possible influences on ooid deposition and distribution, tectonics, specifically flexural mechanisms and folds, are the most important in these shallow basins. Lomando (1999) documented the variations of Holocene onshore facies distributions and near shore ooid factories

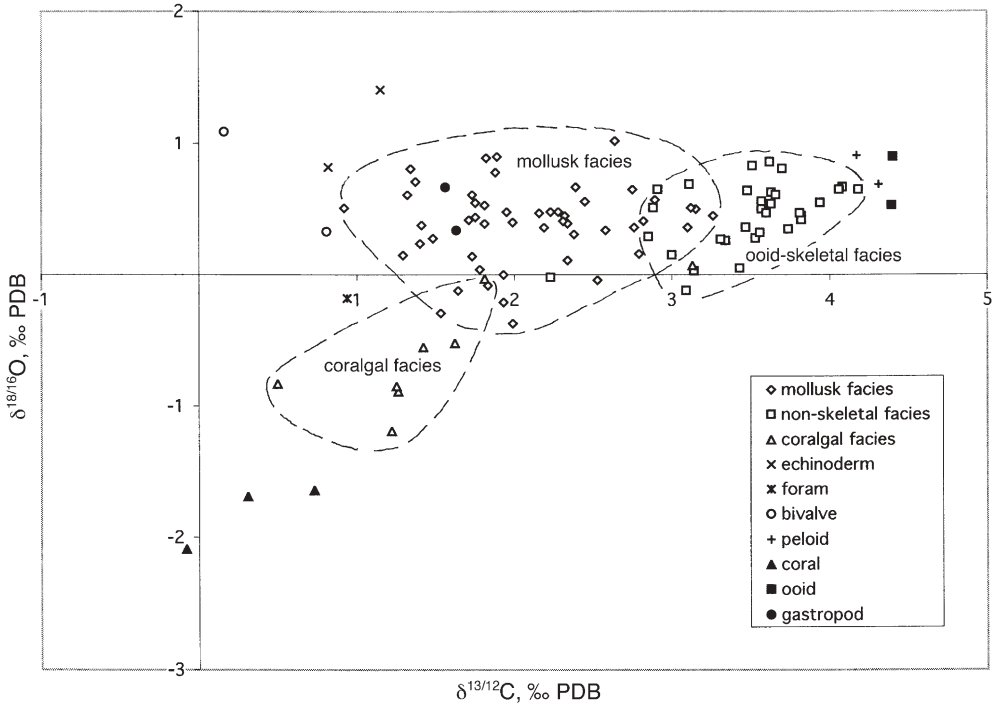

Fig. 12 Scatterplot of the isotope data of bulk samples and end members. Individual facies form separate herds. Note how end members gastropods plot within mollusk facies field; bivales, echinoderms, and foraminifera plot to the left of mollusk facies field. Ooids and peloids plot to the right of non-skeletal field. Corals plot to the lower left of coralgal facies field

Table 8 Correlation matrix of isotope and mineralogy data (upper value is r; statistically significant correlation at p<0.05)

	LMC	ARA	DOL	HMC	δ13C	δ18O
LMC	1 p<.000					
ARA	–.93246 p<0.000	1 p<.000				
DOL	.90218 p<0.000	–.82611 p<0.000	1 p<.000			
HMC	.51983 p<0.000	–.79166 p<0.000	.39547 p<0.000	1 p<.000		
δ13C	–.59433 –.72818 p<0.000 p<0.000	.72520 1 p<0.000 p<.000	–.43327 p<0.000			
δ18O	–.54024 –.38271 p<0.000 p<0.000	.55785 .55529 p<0.000 p<0.000	–.59234 1 p<0.000 p<.000			

in Kuwait and interpreted their control by fold and fault structures. Northeast plunging anticlines created the headlands at Ras Al-Julayah, Ras Al-Zour, and at Ras Bard-Halq near Al-Khafji just across the border in northern Saudi Arabia. The coast-perpendicular shallow faults in southern Kuwait are responsible for the ooid shoals at Nuwaisib south of Al-Khiran. That study also demonstrated that structural underpinnings controlled the locations of oolite beach-dune strand plains, re-entrant coastal ridges, and non-continuous channel-lagoon-sabkha complexes in a repetitive and therefore predictable pattern. The present offshore mapping study complements earlier work and more fully characterizes the Holocene-modern system. Lomando (1998) compared the wave-dominated Kuwait system to the classic linear trends seen in the tide-dominated ramp model developed in the Abu Dhabi region of the UAE. Those comparisons range from inlet frequencies to the distribution of sabkhas. The Kuwait and UAE models, taken together, serve to document the range of inner ramp models that could be expected when mapping ancient sequences.

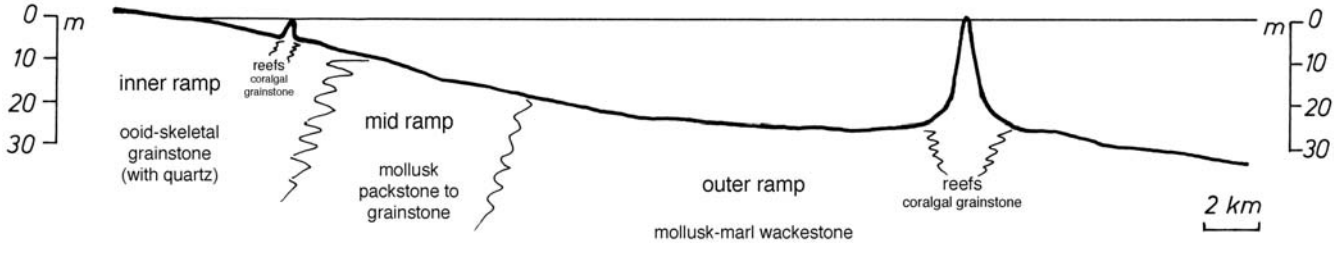

Fig. 13 Schematic profile across the southern Kuwait ramp including occurrence of sedimentary facies

Conclusions

- Five carbonate facies are distinguished on the modern ramp offshore southern Kuwait, NW' Arabian-Persian Gulf. They include (1) inner ramp ooid-skeletal grainstone, (2) rare inner ramp (nearshore) quartz-ooid sand, (3) mid ramp mollusk packstone to grainstone, (4) outer ramp mollusk-marl wackestone, and (5) coralgal grainstone occurring in inner ramp shoal and outer ramp pinnacle reef settings. Facies boundaries are roughly parallel to bathymetric contours and indicate that wave energy largely controls facies distribution.
- Carbonate facies may be distinguished geochemically based on carbon and oxygen isotope composition of bulk samples. Even so, wide ranges in $\delta^{13}C$ and $\delta^{18}O$ isotopic compositions are observed. This observation has important implications for the use of bulk samples taken along sections through ancient ramps and platforms for isotope stratigraphy and paleo-environmental interpretations.
- The NW Arabian-Persian Gulf ramp of Kuwait may serve as a model for a number of ancient ramp examples, just as the classic, yet different ramp system in the SW Gulf area of the UAE.

Acknowledgements We thank the "Holocene Team" (Meshary Ameen, Abdul Aziz Sajer, Aref Al-Doheim, and Meshal Al-Wadi of Kuwait Oil Company, KOC) for assistance during sample collection. Mr. Menahi Al-Anzi and Mr. Khalid Al-Sumati of KOC are also thanked for the many levels of support they provided during the offshore field sampling campaigns. Sandra Hübscher and Stefan Koch (Frankfurt) helped with sample preparations. Alfred Schaub (Frankfurt) made the carbonate analyses, Rainer Petschick (Frankfurt) ran the X-ray diffractometer, and Jens Fiebig (Frankfurt) made the isotope analyses. The financial support of ChevronTexaco Overseas Petroleum, Kuwait, and Kuwait Oil Company is gratefully acknowledged. We thank Sal Mazzullo (Wichita), Isabel Montañez (Davis), and Gene Rankey (Miami) as well as journal reviewers Maurice Tucker (Durham) and Steve Kershaw (Uxbridge) for their helpful comments, which improved the manuscript.

References

Ahr WM (1973) The carbonate ramp: an alternative to the shelf model. Gulf Coast Assoc Geol Soc Trans 23:221–225

Ahr WM (1998) Carbonate ramps 1973–1996: a historical review. In: Wright VP, Burchette TP (eds) Carbonate ramps. Geol Soc Spec Publ 149:7–14

Al-Bakri D, Al-Ghadban A (1984) Mineralogy, genesis, and sources of surficial sediments in the Kuwait marine environment, northern Arabian Gulf. J Sediment Petrol 54:1266–1279

Al-Ghadban AN (1990) Holocene sediments in a shallow bay, southern coast of Kuwait, Arabian Gulf. Mar Geol 92:237–254

Al-Sarawi M, Al-Zamel A, Al-Tafaiy IA (1993) Late Pleistocene and Holocene sediments of the Khiran area (South Kuwait). J Univ Kuwait (Science) 20:145–156

Baltzer F, Purser BH (1990) Modern alluvial fan and deltaic sedimentation in a foreland tectonic setting: the lower Mesopotamian Plain and the Arabian Gulf. Sediment Geol 67:175–197

Burchette TP, Wright VP (1992) Carbonate ramp depositional systems. In: Sellwood BW (ed) Ramps and reefs. Sediment Geol 79:3–57

Cann RS (1962) Recent calcium carbonate facies of the north-central Campeche Bank, Yucatan, Mexico. PhD thesis Columbia Univ., 127 pp (unpublished)

Carpenter KE, Harrison PL, Hodgson G, Alsaffar AH, Alhazeem SH (1997) The corals and coral reef fishes of Kuwait. Kuwait Inst Sci Res, 166 pp

Cozzi A, Allen PA, Grotzinger JP (2004) Understanding carbonate ramp dynamics using $\delta^{13}C$ profiles: examples from the Neoproterozoic Buah Formation of Oman. Terra Nova 16:62–67

Downing N (1985) Coral reef communities in an extreme environment: the northwestern Arabian Gulf. Proc 5th Int Coral Reef Symp 6:343–348

Drzewiecki PA, Simo JA (1997) Carbonate platform drowning and oceanic anoxic events on a mid-Cretaceous carbonate platform, south-central Pyrenees, Spain. J Sediment Res 67:698–714

Duane MJ, Al-Zamel AZ (1999) Syngenetic textural evolution of modern sabkha stromatolites (Kuwait). Sediment Geol 127:237–245

Dunham RJ (1962) Classification of carbonate rocks according to depositional texture. In: Ham WE (ed) Classification of carbonate rocks. Am Assoc Petrol Geol Mem 1:108–121

Emery KO (1956) Sediments and water of Persian Gulf. Bull Am Assoc Petrol Geol 40:2354–2383

Enos P, Sawatsky LH (1981) Pore networks in Holocene carbonate sediments. J Sediment Petrol 51:961–985

Etterson FR (1993) Possible flexural controls on the origins of extensive ooid-rich carbonate environments of the United States. In: Keith BD, Zuppann CW (eds) Mississippian oolites and modern analogues. Am Assoc Petrol Geol Stud Geol 35:13–30

Evans G (1966) The recent sedimentary facies of the Persian Gulf Region. Phil Trans R Soc Lond A259:291–298

Evans G, Kinsman DJJ, Shearman DJ (1964) A reconnaissance survey of the environment of recent carbonate sedimentation along the Trucial Coast, Persian Gulf. In: van Straaten MJU (ed) Deltaic and shallow marine deposits. Dev Sedimentol 1:129–135

Ferreri V, Weissert H, D'Argenio B, Buonocunto FP (1997) Carbon isotope stratigraphy: a tool for basin to carbonate platform correlation. Terra Nova 9:57–61

Gould HR, Stewart RH (1955) Continental terrace sediments in the northeastern Gulf of Mexico. In: Hough JL (ed) Finding ancient shorelines. Soc Econ Min Paleont Spec Publ 3:2–20

Grötsch J, Billing I, Vahrenkamp V (1998) Carbon-isotope stratigraphy in shallow-water carbonates: implications for Cretaceous black-shale deposition. Sedimentology 45:623–634

Gunatilaka A (1986) Kuwait and the northern Arabian Gulf: a study in Quaternary sedimentation. Episodes 9:223–231

Gunatilaka A (1991) Dolomite formation in coastal Al-Khiran, Kuwait, Arabian Gulf—a re-examination of the sabkha model. Sediment Geol 72:35–53

Handford CR (1988) Review of carbonate sand-belt deposition of ooid grainstones and application to Mississippian reservoir, Damme field, southwestern Kansas. Am Assoc Petrol Geol Bull 72:1184–1199

Harris CD, Freuenfelter GH (1993) Depositional Aspects of the Golconda Group (Chesterian) Oolite Bodies, Southwestern Illinois basin. In: Keith BD, Zuppann CW (eds) Mississippian oolites and modern analogues. Am Assoc Petrol Geol Stud Geol 35:129–140

Houbolt JJHC (1957) Surface sediments of the Persian Gulf near the Qatar Peninsula. PhD Thesis Univ Utrecht, Mouton & Co, The Hague, 113 pp

Immenhauser A, Della Porta G, Kenter JAM, Bahamonde JE (2003) An alternative model for positive shifts in shallow-marine carbonate $\delta^{13}C$ and $\delta^{18}O$. Sedimentology 50:953–959

Jenkyns HC (1995) Carbon-isotope stratigraphy and paleoceanographic significance of the lower Cretaceous shallow-water carbonates of Resolution Guyot, mid-Pacific mountains. In:

Winterer EL, Sager WW, Firth JV, Sinton JM (eds) Proc Ocean Drilling Prog, Sci Res 143:99–104
Jones MR (1987) Surficial sediments of the western Gulf of Carpentaria, Australia. Austral J Mar Freshw Res 38:151–167
Kendall CGSC, Skipwith PAd'E (1969) Geomorphology of a recent shallow-water carbonate province: Khor Al Bazam, Trucial Coast, southwest Persian Gulf. Geol Soc Am Bull 80:865–892
Khalaf FI (1988) Quaternary calcareous hard rocks and the associated sediments in the intertidal and offshore zones of Kuwait. Mar Geol 80:1–27
Khalaf FI, Ala M (1980) Mineralogy of the recent intertidal muddy sediments of Kuwait—Arabian Gulf. Mar Geol 35:331–342
Khalaf FI, Al-Bakri D, Al-Ghadban A (1984) Sedimentological characteristics of the surficial sediments of the Kuwaiti marine environment, northern Arabian Gulf. Sedimentology 31:531–545
Khalaf FI, Al-Ghadban A, Al-Saleh S, Al-Omran L (1982) Sedimentology and mineralogy of Kuwait Bay bottom sediments, Kuwait—Arabian Gulf. Mar Geol 46:71–99
Kinsman DJJ (1969) Interpretation of Sr^{2+} concentrations in carbonate minerals and rocks. J Sediment Petrol 39:486–508
Kirkham A (1998) A Quaternary proximal foreland ramp and its continental fringe, Arabian Gulf, UAE. In: Wright VP, Burchette TP (eds) Carbonate ramps. Geol Soc Spec Publ 149:15–41
Land LS (1989) The carbon and oxygen isotopic chemistry of surficial Holocene shallow marine carbonate sediment and Quaternary limestone and dolomite. In: Fritz P, Fontes JC (eds) Handbook of environmental isotope geochemistry. Elsevier, Amsterdam, 3:191–217
Logan BW, Harding JL, Ahr WM, Williams JD, Snead RG (1969) Late Quaternary carbonate sediments of Yucatan shelf, Mexico. Am Assoc Petrol Geol Mem 11:5–128
Lomando AJ (1998) Holocene wave-dominated ramps: new exploration models from Kuwait-Saudi Arabian coast of the northern Arabian Gulf and the northern Yucatan, Mexico, with a comparison to siliciclastic systems. Am Assoc Petrol Geol, Ext Abstr Figs, p. A410, 1–3
Lomando AJ (1999) Structural influences on facies trends of carbonate inner ramp systems, examples from the Kuwait-Saudi Arabian coast of the Arabian Gulf and northern Yucatan, Mexico. GeoArabia 4:339–360
Loreau J-P (1982) Sédiments aragonitiques et leur genèse. Mém Mus Nat d'Hist Nat Nouv Sér C 47:312 pp
Manley RD, Choquette PW, Rosen MB (1993) Paleogeography and cementation in a Mississippian oolite shoal complex: Ste. Genevieve Formation, Willow Hill Field, Southern Illinois Basin. In: Keith BD, Zuppann CW (eds) Mississippian oolites and modern analogues. Am Assoc Petrol Geol Stud Geol 35:91–114
Milliman JD (1974) Recent sedimentary carbonates. Part 1. Marine carbonates. Springer, Berlin Heidelberg New York, 375 pp
Mutti M, Bernoulli D, Stille P (1997) Temperate carbonate platform drowning linked to Miocene oceanographic events: Maiella platform margin, Italy. Terra Nova 9:122–125
Patterson WP, Walter LM (1994) Depletion of ^{13}C in seawater $\sum CO_2$ on modern carbonate platforms: significance for the carbon isotopic record of carbonates. Geology 22:885–888
Picha F (1978) Depositional and diagenetic history of Pleistocene and Holocene oolitic sediments and sabkhas in Kuwait, Persian Gulf. Sedimentology 25:427–450
Purser BH (ed) (1974) The Persian Gulf. Holocene carbonate sedimentation and diagenesis in a shallow epicontinental sea. Springer, Berlin Heidelberg New York, 471 pp
Read JF (1985) Carbonate platform facies models. Bull Am Assoc Petrol Geol 69:1–21
Robinson BW, Gunatilaka A (1991) Stable isotope studies and the hydrological regime of sabkhas in southern Kuwait, Arabian Gulf. Sediment Geol 73:141–159
Uchupi E, Swift SA, Ross DA (1996) Gas venting and late Quaternary sedimentation in the Persian (Arabian) Gulf. Mar Geol 129:237–269
Vahrenkamp VC (1996) Carbon isotope stratigraphy of the upper Kharaib and Shuaiba Formations: implications for the early Cretaceous evolution of the Arabian Gulf region. Am Assoc Petrol Geol Bull 80:647–662
Vallardes I, Recio C, Lendinez A (1996) Sequence stratigraphy and stable isotopes ($\delta^{13}C$, $\delta^{18}O$) of the late Cretaceous carbonate ramp of the western margin of the Iberian chain (Soria, Spain). Sediment Geol 105:11–28
Wagner CW, van der Togt C (1973) Holocene sediment types and their distribution in the southern Persian Gulf. In: Purser BH (ed) The Persian Gulf. Springer, Berlin Heidelberg New York, pp 123–155
Walkden G, Williams A (1998) Carbonate ramps and the Pleistocene-Recent depositional systems of the Arabian Gulf. In: Wright VP, Burchette TP (eds) Carbonate ramps. Geol Soc Spec Publ 149:43–53
Weber JN (1967) Factors affecting the carbon and oxygen isotopic composition of marine carbonate sediments—Part I, Bermuda. Am J Sci 265:586–608
Weber JN, Woodhead PMJ (1969) Factors affecting the carbon and oxygen isotopic composition of marine carbonate sediments—II. Heron Island, Great Barrier Reef, Australia. Geochim Cosmochim Acta 33:19–38
Wilson JL (1975) Carbonate facies in geologic history. Springer, Berlin Heidelberg New York, 471 pp
Wissler L, Funk H, Weissert H (2003) Response of early Cretaceous carbonate platforms to changes in atmospheric carbon dioxide levels. Palaeogeogr Palaeoclimatol Palaeoecol 200:187–205
Wright VP, Burchette TP (1998) Carbonate ramps: an introduction. In: Wright VP, Burchette TP (eds) Carbonate ramps. Geol Soc Spec Publ 149:1–5